

8501

UNCLASSIFIED

NRL Report 4382
Copy No. 67



INVESTIGATION OF A PULSED-LIGHT IFF SYSTEM FOR USE BETWEEN AN AIRCRAFT AND A SUBMARINE



D. F. Hansen, W. S. Plymale, Jr.,
and G. L. Stamm

Photometry Branch
Optics Division

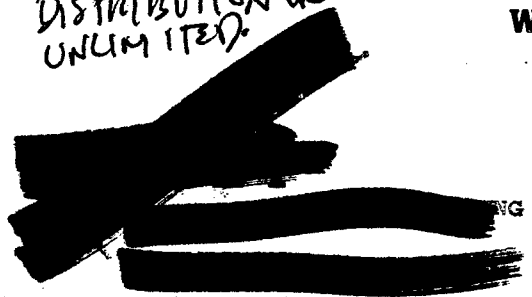
DECLASSIFIED: By authority of
OPNAVINST 5510.1 H, 29 APR 88
Date
Site Authority C. Rodgers 1221
Entered by NRL Code

July 28, 1954

CLASSIFIED BY [REDACTED] DEC [REDACTED]
[REDACTED]
[REDACTED]
[REDACTED]

FR-4382-67 AD 044287
Investigation of a Pulsed-Light IFF
NRL-FR-4382
Confidential Report
Controlled by Code 5227

APPROVED FOR PUBLIC RELEASE
DISTRIBUTION OR UNLIMITED
NAVAL RESEARCH LABORATORY
Washington, D.C.



PLEASE RETURN THIS COPY TO:
NAVAL RESEARCH LABORATORY
WASHINGTON, D.C. 20390
ATTN: CODE 2028
Because of our limited supply you are requested to return this copy as soon as it has served your purposes so that it may be made available to others for reference use. Your cooperation will be appreciated.
NDW-NRL - 5070/2035 (10-67)

CONTENTS

Abstract	ii
Problem Status	ii
Authorization	ii
INTRODUCTION	1
SEA WATER AND THE ELECTROMAGNETIC SPECTRUM	2
AN OPTICAL IDENTIFICATION SYSTEM	5
EXPERIMENTAL TRANSMITTER	14
EXPERIMENTAL RECEIVER	22
RESULTS	29
DISCUSSION	39
ACKNOWLEDGMENTS	40
REFERENCES	41
DISTRIBUTIONS	44

ABSTRACT

A need exists in antisubmarine warfare for an aircraft-submarine IFF system. The most promising wavelength region for IFF operation appears to be in the visible wavelengths, or in the near-ultraviolet when visual security is necessary. In these spectral regions, the ocean and coastal water classifications of Jerlov are a compact summary of the known transmission characteristics of the world's sea water.

Because of its versatility, a completely physical IFF system is preferred to a visual or semivisual system. A somewhat simplified theory is used for a physical system whose principal components are a flashtube transmitter and a photoelectric receiver. In this theory, the parameters of the system are related to the many variables present. The theory sets limiting signal-to-noise ratios necessary for positive operation of the IFF system under day or night conditions in any type of ocean water. Experimental transmitters and receivers have been built embodying most of the desirable features for signal work of this type, and the behavior of their parameters has been investigated in detail. Daytime bidirectional shipboard experiments were conducted at sea under various sunlight conditions. When the transmitter was submerged in the Gulf Stream, the signal was detectable to a depth of 382 feet. Experimentation also demonstrated the equivalence of signaling in either direction. Comparison of the calculated results with the experimental results showed the use of the limiting equations to be justified. The equations have been applied to the basic problems of an IFF system. In the absence of moonlight on tropical or subtropical waters, results show positive operation to be possible for aircraft heights to 600 meters and submarine depths to 50 meters both in the visible and near ultraviolet. Daytime operation is not possible as an IFF system with the present equipment. Improvements in the equipment and increased flash intensity, however, may eventually give a positive operating system under any circumstances.

PROBLEM STATUS

This is an interim report; work on the shipboard phase of the problem is concluded, but planning for direct submarine-aircraft measurements and equipment improvements is still in progress.

AUTHORIZATION

NRL Problem N03-22
Project NR 473-220

Manuscript submitted May 25, 1954



INVESTIGATION OF A PULSED-LIGHT IFF SYSTEM FOR USE BETWEEN AN AIRCRAFT AND A SUBMARINE

INTRODUCTION

A series of investigations has been conducted at the Naval Research Laboratory to explore the possible naval use of ultraviolet light as a means of optical communication and identification between an aircraft or surface vessel and a submerged submarine. Previous reports (1,2) describe shipboard findings on the nighttime transmission of ultraviolet light through sea water and the air-sea boundary. These experiments were performed to obtain data for an evaluation of a possible nonvisible nighttime identification system. Attenuation measurements were made on the pulse amplitude of an ultraviolet signal from a submerged transmitter lowered to a cable depth limitation of 200 feet. The basic components of the system consisted of a large spiral flashtube in the transmitter and a photomultiplier tube in the receiver. Signal measurements were made on an oscilloscope display. The work was unidirectional, and no attempt was made to transmit to a submerged receiver from a shipboard transmitter.

In August 1953, improved equipment and visible light were used in making bidirectional daylight measurements aboard the E-PCE(R) 851 enroute from NRL to Panama City, Florida. An entirely new instrumentation was effected for this trip. Most of the mechanical changes suggested themselves during the shipboard use of the previous equipment. The electronic changes were intended to improve the signal-to-noise (S/N) ratio and, hence, performance of the new equipment operating as a submarine-aircraft identification system. Reception ranges were indicative of the possible eventual development of a workable system for both day and night operation.

To determine the feasibility of a system that would be completely reliable under most circumstances, a rather extensive knowledge is required of the many influencing variables. The principal factor of influence is, of course, the signal transmission in the many types of water in which a submarine may operate. Other variables such as the amount of sunlight or moonlight present, atmospheric attenuation, aircraft altitude, and submarine depth all play a part to a great or lesser extent.

The discussion is facilitated if it is confined to certain limiting cases, viz., a fixed aircraft altitude, at times a fixed submarine depth, and also the best and possibly the worst values of the other influencing variables. The chosen values of the aircraft altitude and submarine depth are unlikely to be exceeded in actual operation of the system.

General equations will first be derived to relate the characteristics of sea water and the other variables to the system parameters. Restrictions are then placed upon certain of the variables and parameters to obtain the defining expressions for positive operation of day and night identification systems. In an effort to establish the reliability of

calculations, experimental signal-to-noise ratios for a particular wavelength and specified conditions are compared to calculated signal-to-noise ratios under similar circumstances. Once established, the equations are applied to the problems of an IFF (Identification Friend or Foe) system. The findings are sufficiently general and with but a slight modification are directly applicable to a submarine-aircraft communication system.

The nature of the identification system interrelates a number of seemingly diverse topics, i.e., sea water, flash discharges, and electronic noise problems. For the sake of completeness, all are treated in this report. The discussion is best begun with a presentation of the accumulated knowledge of sea water characteristics and their relation to the subject at hand.

SEA WATER AND THE ELECTROMAGNETIC SPECTRUM

Evidence compiled over many years by those interested in the optics of sea water has shown that oceans and their currents each have a constancy of transmission which may be modified to some extent by the seasons, concentration of plankton, and weather. In coastal waters, however, there are additional divergencies of transmission due to contaminants and a peculiar "yellow substance."

A well-known region of high transmittance, or "window," for electromagnetic radiation in sea water is centered in the visible section of the optical wavelengths. It is toward exploring the possible use of this window that most of the present work has been directed.

When it is considered necessary to maintain security while using a nighttime identification system, the visible section of the window is unlikely to be used. Because of its higher transmission values, the near-ultraviolet optical region was chosen for nonvisible nighttime use early in the investigation in preference to the near-infrared region. In daytime, or when visible security is unnecessary at nighttime, the visible wavelengths need not be excluded from possible use. Although sea water attenuates least at the visible wavelengths, the region of optimum daytime operation has additional determining factors, among which are the sunlight and flashtube spectral energy distributions.

The transmission of electromagnetic waves in sea water and pure water over a broad frequency range is shown in Fig. 1. Composed of data taken from the literature (3 through 10), these curves were used to explore the possibility that another window in the spectrum may have been overlooked for use. Some regions of the curves are averaged from the results of many investigators; in others there are little or no data available. In addition to the previously described natural causes of variations in sea water transmission, there is genuine disagreement among investigators on transmission values, particularly in the radio region where difficulty exists in interpreting the measurements. Thus, this curve taken alone is accurate to only slightly more than an order of magnitude for transmission values, but this order is sufficient for its intended purpose.

Because there are large gaps in the sea water spectrum, the curve from available data on pure water is also shown. In the regions where sea water data are lacking, the pure water curve can be taken as an approximate upper limit to the sea water transmission. Although gaps are also present in this curve, the trends are distinguishable.

Steepness of the curve in the immediate vicinity of the visible region is due to the manner of presentation which has the logarithm of the transmission per meter plotted on

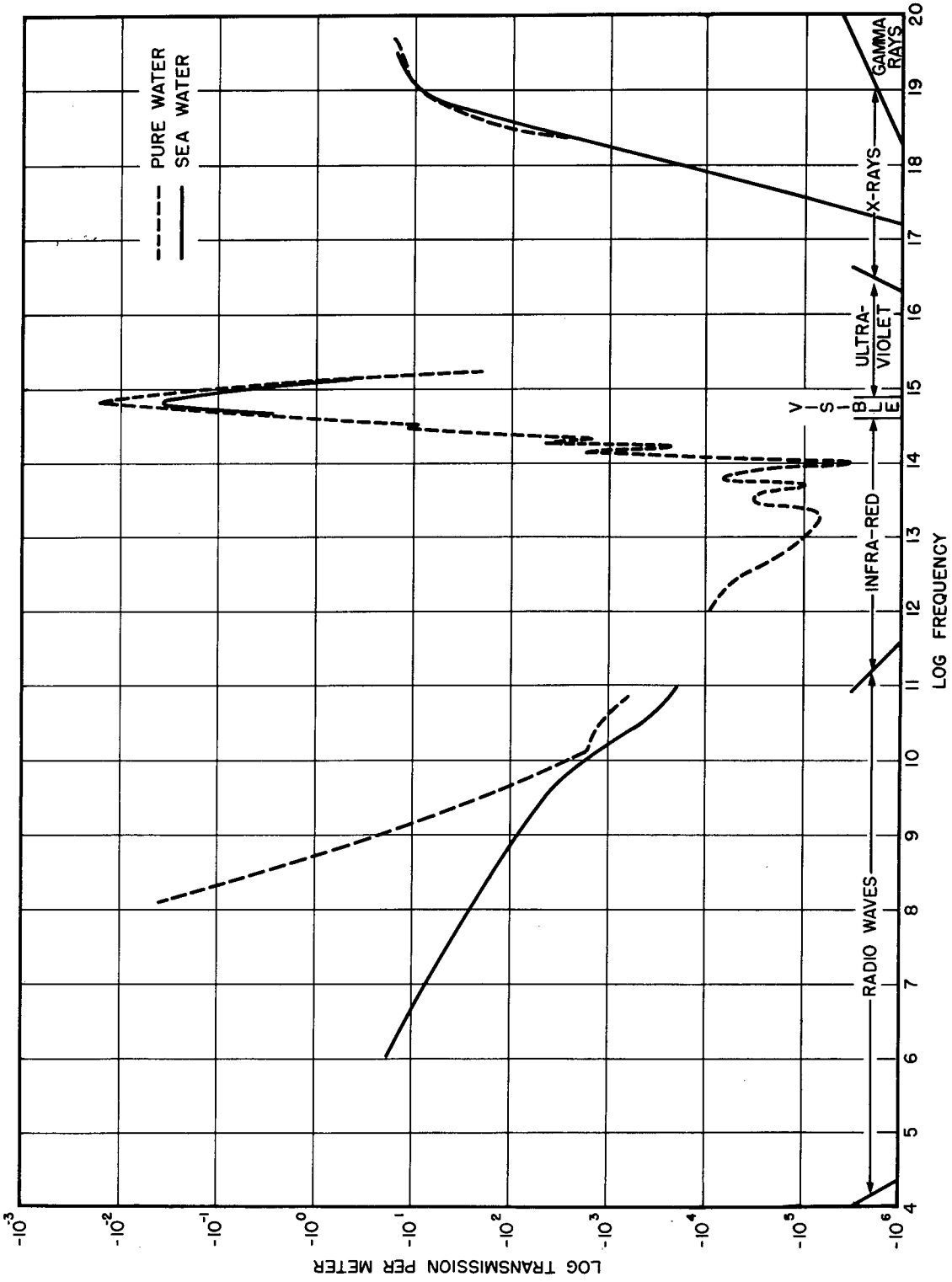


Fig. 1 - Transmission of electromagnetic radiations in sea water and pure water

a logarithmic scale. The fall-offs beyond the near-infrared and near-ultraviolet regions are actually precipitous. The transmission after leaving this central peak does not rise again to a value of 10 percent per meter ($\log T = -1$) in the conceivably useful frequency range. A little reflection will show that a value of transmission as low as 10 percent per meter will be prohibitive for signaling over a moderate distance through sea water since the attenuation will go as 10^n , where n is the number of meters traversed. Where this value is approached in the long radio wave and gamma-ray regions, there are obvious added difficulties of a mechanical nature associated with any system. It may thus be concluded that only the optical wavelengths, and in particular only those whose transmittance is well above 10 percent per meter, need be considered for possible use when signaling through reasonable distances in sea water. Rauen (11) recently demonstrated that it is possible to communicate with long-wavelength radio waves in certain submarine applications where only several feet of water are involved.

In a study of sea water, Jerlov (4,12) proposed a series of normal transmission curves for different types of coastal waters and similarly for different types of ocean waters. They, being the most recent and comprehensive of several sea water classifications, will be used throughout this discussion. His classification for coastal waters (curves for five of the nine types are shown in Fig. 2) is based on experiments conducted in the Baltic, Skagerrak, Gullmarfjord, Norwegian Fjords, and off the North American Pacific coast. He considers these curves as typically representative of coastal water in the Temperate Zone. This schema as well as that for ocean waters, based on considerable evidence as they are, remain in need of verification for many of the waters in which submarines could operate. A particularly important need, as it later develops, are the relations between coastal depths and water types.

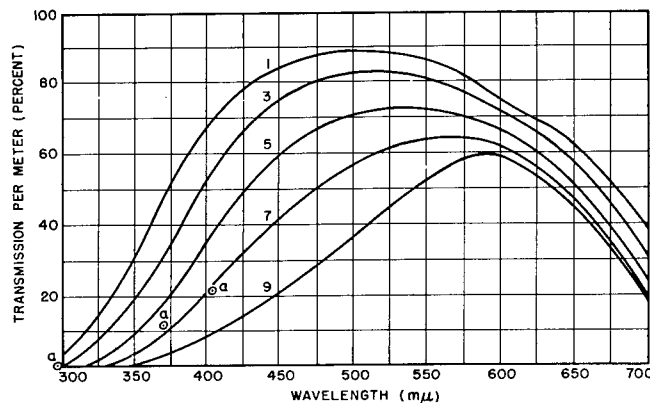
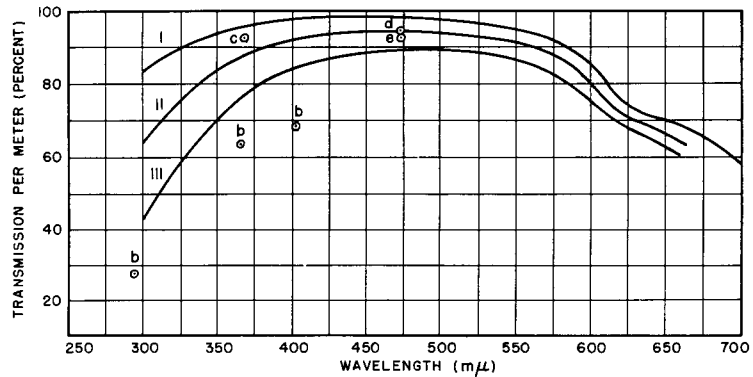


Fig. 2 - Normal transmission curves for different types of coastal water -- after Jerlov (Ref. 4)

The heavy absorption in the ultraviolet region is, according to Kelle (13), due to a "yellow substance" which originates from carbohydrates usually found in phytoplankton. The yellow substance is abundant in coastal waters and chiefly responsible for their green color.

To establish the classification of particular coastal or ocean waters, it is sufficient when using these curves to find the transmission at only one wavelength except at locales with contaminants that show selective absorption. Jerlov claims reasonable agreement for the entire transmission curve if the transmission at a wavelength in the violet or near ultraviolet is determined.

Fig. 3 - Normal transmission curves for different types of ocean water -- after Jerlov (Ref. 4)



As shown in Fig. 3, Jerlov has classified ocean water into three types. Curve I is representative of the clearest ocean waters such as the Sargasso and eastern Mediterranean Seas, whereas Curve II is characteristic of ocean waters of relatively high turbidity. It is between Curves I and II that most tropical and subtropical waters may be classed. In drawing Curve III Jerlov used his own data, the observations recorded by Atkins and Poole (14) in the English Channel, and the data collected by Utterback (15) in the North Pacific Ocean. This curve and the region between it and Curve II should typify northern and temperate waters. By observing these curves it can be seen that increased latitude lowers the transparency of ocean waters. Since Jerlov's measurements rarely exceed a depth of ten meters in the red and ultraviolet, he restricts the classification to the uppermost ten-meter stratum. Most evidence, however, indicates a slight increase of transparency with depth so that the use of the classification at greater depths, if in error, will err toward a safety factor.

Transmission values at various depths are readily obtainable from the results of NRL experiments, and some of these are shown plotted with Jerlov's schema in Figs. 2 and 3. In the waters in which these values were measured (Table 1), all points except those labeled (b) show excellent agreement with the expected values for the described waters. The water in which the excepted values were measured has been interpreted as slope water, i.e., the region where the coastal and ocean types mix. In the only known survey of its kind, Clarke (16) established the delineating boundaries of coastal, slope, and ocean waters for the Northeastern Atlantic. Clarke's classification was made on the basis of attenuation of the total visible light. No attempt, however, is made here to establish the connection between it and Jerlov's classification. A workable identification system -- if it is at all practicable -- must function somewhere in the central optical region of the electromagnetic spectrum. Jerlov's curves are a compact summary of most of what is known about the variations in sea water transmission at these wavelengths. In addition, the classification of much of the world's ocean water is known, and a rough rule of thumb is available to apply it. For coastal waters, however, such is not the case. Although the classification of the Temperate Zone coastal waters is extremely important to this work, the identifications of the types, locations, and depths are equally important. At present, this is impossible because of the meager amount of reliable published data. Jerlov's own published work carries little information of this sort. Since it is likely that submarines can navigate submerged in some of what is classed as coastal water, the relations between depth and coastal water type may become necessary.

AN OPTICAL IDENTIFICATION SYSTEM

There would seem to be only a limited number of practical forms which an identification system of this nature might take. First of all, a temptation might be felt to take

TABLE 1
Classification and Sites of Transmission Measurements
Indicated in Figures 2 and 3

Points	Curve	Water Class	Location		Date
			General	Specific	
a	7	Coastal	Chesapeake Bay		May 1950
b		Slope	Six miles out of Key West harbor	Lat. 24° 27' N Long. 81° 49' W	March 1951
c	I and II	Ocean	Gulf Stream headwaters	Lat. 24° 22' N Long. 81° 49' W	April 1952
d	II	Ocean	Between Gulf Stream and Sargasso Sea 155 mi east of Daytona Beach, Fla.	Lat. 29° 32' N Long. 78° 04' W	August 1953
e	II	Ocean	In Gulf Stream nine miles east of Miami, Fla.	Lat. 25° 55' N Long. 79° 59' W	August 1953

advantage of the high transmission at the visible wavelengths and use the eye as a receiver. If it is assumed that a two-way system is necessary to make identification complete or to have a successful communication system, the visual system presents no difficulty to the aircraft observer, but is entirely unlikely for use by the submarine.

It could be assumed then that the submarine uses, as an alternative, a photoelectric device to receive the interrogating signals from the aircraft and that the reception of the identifying reply aboard the aircraft would remain visual. There remains the problem of nighttime visual security which would limit the usefulness of the system. Any consideration here of a visual or semivisual system has been rejected for these and additional reasons. First, there is no experimental evidence for comparison with a definable system of this sort. The effects of sea state and transparency on visibility of submerged objects are being theoretically and experimentally investigated by Duntley (17) and sea state and surface glitter by Cox and Munk (18). It is felt that evaluation of such a system would require direct submarine-to-aircraft experiments in order to correctly simulate the conditions in the field of view of the observer. Second, a completely physical system is readily defined, and although comparison will be made with shipboard data extrapolated to aircraft heights, it seems susceptible to little error. Again, a semivisual system's signaling range will depend on the time-intensity product of the flash discharge (19), whereas that of an entirely electromechanical system is limited only by the intensity. This fact has some significance when considering fast repetition rates and transmitter size. Further, there is the added advantage of having a single system with provisions for shifting wavelength region of operation for security reasons.

In principle, the two-way physical system amounts to the basic form of a radar IFF system. The similarity is close, and in order to facilitate the discussion, the terminology usually employed in those systems (20,21) will be followed.

- Interrogator — A transmitter used by an operator to challenge a target for identification.
- Transponder — A receiver and transmitter carried by each friendly craft. It automatically transmits an identifying reply whenever it receives a challenge from an interrogator.
- Responder — This equipment serves to detect the transponder's reply.

A conceptual picture of a system using these basic elements is shown in Fig. 4. This system is the only kind achievable with the present slow transmitter flash rate. Little attempt will be made in this discussion to cover the engineering details of such a system. The concern here is mainly with the parameters which will determine the effectiveness of operation. In this respect equations are needed to relate these parameters to the factors limiting transmission. To simplify the discussion, a number of approximations are used, and their validity must be assumed for most circumstances.

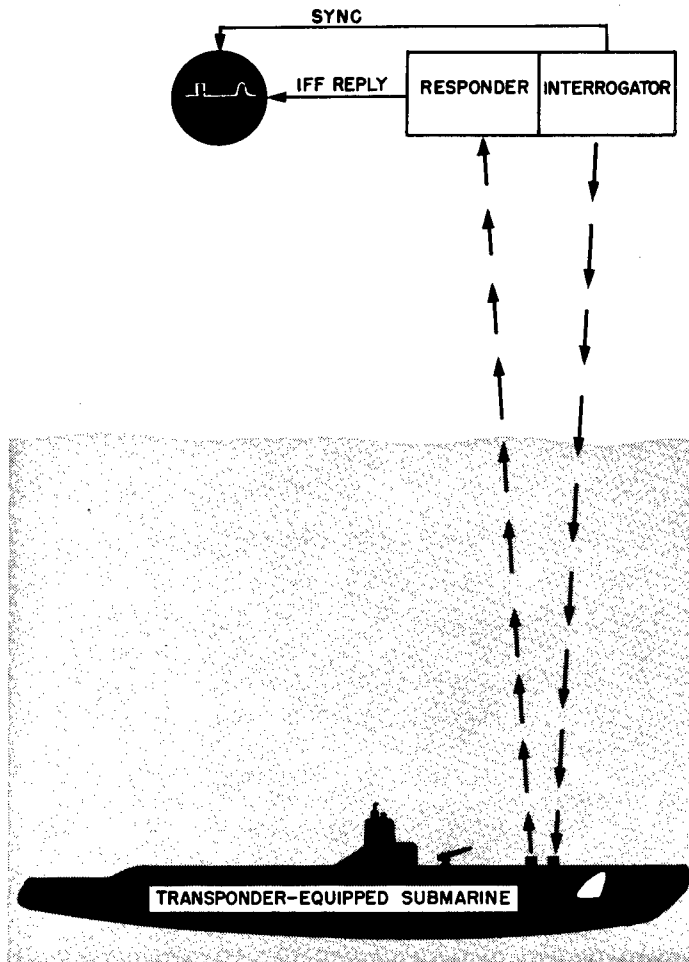


Fig. 4 - Diagram of a basic IFF system showing a reply to a challenge

The mathematical treatment is restricted to the case where the submarine-to-aircraft line of sight is normal to the plane of the ocean surface.

Over the distances involved the transmitters can conveniently be considered as point sources of radiation. Thus, neglecting any aureole effects, let the time-varying spectral radiant intensity of the interrogator flash be represented by $J_I(\lambda, t)$. This signal, in traveling to the transponder, is attenuated by the inverse square law and the absorption and scattering per unit length of path in air and water. The approximate spectral irradiance $H_I(\lambda, t)$ at the transponder due to the interrogating source is

$$H_I(\lambda, t) = \frac{J_I(\lambda, t) \exp(-\alpha(\lambda)r_a - \beta(\lambda)r_s)}{(r_a + r_s)^2} \quad (1)$$

where

$H_I(\lambda, t)$ = Spectral irradiance at the transponder due to the interrogator
(watts/meter² x 10 m μ)

$J_I(\lambda, t)$ = Equivalent beam spectral radiant intensity
(watts/steradian x 10 m μ bandwidth)

r_a = Signal range in air (meters)

r_s = Signal range in sea water (meters)

$\alpha(\lambda)$ = Total attenuation coefficient in air (meters⁻¹)

$\beta(\lambda)$ = Total attenuation coefficient in sea water (meters⁻¹).

Any attenuation effects due to the sea state and any loss resulting from reflection at the surface are neglected in Eq. (1). From refractive indices of sea water (9) and Fresnel's formula, it can be easily seen that the losses due to reflection by a calm sea amount to at most only a few percent over the entire spectral region of interest. Sea state effects have not been quantitatively investigated, but shipboard experience has shown that even with moderate seas running there is little signal attenuation.

It is next assumed that the receiver section of the transponder presents a phototube with a sensitive area (A meters²) normal to the direction of the interrogator; the average cathode spectral sensitivity of the phototube is $S(\lambda)$ amperes per watt. For comparison with experimental data a current multiplying factor m arising from the use of a photo-multiplier tube will be included. There is then $AH_I(\lambda, t)$ watts per 10 m μ bandwidth of power at the photocathode and an available signal current of $mAH_I(\lambda, t)S(\lambda)$ amperes at the anode. An optical filter of transmittance $T(\lambda)$ will usually be present and a "gain" factor $g(\lambda)$ is needed to account for the enhancement of signal flux on the photocathode due to the employment of an optical system. The signal current $I_T(t)$ available for amplification by the transponder is then given by

$$I_T(t) = \int_0^{\infty} A m g(\lambda) T(\lambda) S(\lambda) H_I(\lambda, t) d\lambda \quad (2)$$

where

$I_T(t)$ = Signal current at anode of transponder phototube (amps)

A = Area of photocathode (meters²)

m = Current multiplying factor

$g(\lambda)$ = Signal flux enhancement factor (gain of receiver optical system)

$T(\lambda)$ = Transmittance of receiver filter

$S(\lambda)$ = Spectral sensitivity of photocathode (amps/watt).

We shall not introduce a general expression for evaluating the factor $g(\lambda)$ since no optics were employed in the experimental receiver. It is included as a systems parameter to show a possible means of increasing the signal current.

There will be a minimum signal-current amplitude required at the input to the amplifier to trigger off the transmitter in answer to an interrogation. This limit is determined by the noise characteristics of the receiver.

Combination photomultiplier-electronic amplifier devices such as comprise the receiver are likely to have a great many noise sources present. Because of the nature of the measurements, only four noise sources (22) are considered here.

1. The thermal agitation noise in a resistor, or Johnson noise,
2. Normal shot noise present in thermionic emission of the photocathode,
3. A form of shot noise due to the random rate of arrival of photons at the photocathode, and
4. Noise due to the glitter of sunlight reflecting off the water.

Goldstein (23) found the frequency spectrum of the type (4) noise to be limited to the very low frequencies. By proper bandwidth choice for the radiation receiver, this type is eliminated as a possible noise source. The remaining sources have a Gaussian or "white spectrum" nature. Since random noise adds quadratically, that part of the total mean square noise current $(\bar{I})^2$ present in the average anode current $(\bar{I}_D + \bar{I}_N)$ defining the receiver limitation will be

$$(\bar{I})^2 = \left[\frac{4kT}{R} + 2 me (\bar{I}_D + \bar{I}_N) \right] \cdot B \quad (3)$$

where

k = Boltzman's constant (erg x degree⁻¹)

T = Absolute temperature of the anode resistor (degrees K)

R = Anode load resistor (ohms)

m = Current multiplication factor

e = Electron charge 1.59×10^{-19} coulombs

I_D = Average anode direct current (amps)

I_N = Average anode dark current (amps)

B = Receiver frequency bandwidth (between half-power points) (sec^{-1})

$\frac{4kTB}{R}$ = Johnson noise

$2meI_D B$ = Photon random rate of arrival noise

$2meI_N B$ = Thermionic shot noise.

Some caution is necessary in the determination and application of the bandwidth factor B . It is apparent from Eq. (3) that reduction of receiver bandwidth brings about a reduction of the noise. To a certain extent, an increase in signal-to-noise ratio may thus be effected, since there is an optimum bandwidth for maximum signal-to-noise ratio. A discussion of this optimum bandwidth and the other limitations on B is postponed until the analysis of the design of the experimental receiver.

Further consideration of the noises (22,24) shows that Johnson noise will be masked over by one or the other of the remaining noise sources, depending on whether it be day or night. Under ideal nighttime conditions the only source of noise will be the shot noise in the dark current, if it is assumed that the full gain of the multiplier phototube is used. Any discussion of the case where photon and shot noises are of comparable magnitude can be omitted since it would represent only a small time period on the day-night illumination scale. The photon noise then is the daytime and twilight limiting factor and shot noise that of nighttime. The mean square current values of day noise is given by

$$(\bar{I})^2 = 2me\bar{I}_D B \quad (4)$$

and similarly the value of night noise is given by

$$(\bar{I})^2 = 2me\bar{I}_N B. \quad (5)$$

The minimum amount of signal required for operation in the presence of these noises will be determined by the amount of spurious triggering allowable in the transponder. If the transponder has a given triggering level set by $I_1 = \hat{I}_1$ then there is a finite probability that some noise peak will exceed this level. Since noise is a random phenomenon, a noise peak of any predetermined value can be observed if a long enough period of time is allowed to elapse. For broadband noise with Gaussian frequency distribution, the expected number of current peaks per second $n(\hat{I}_1)$ in excess of the triggering level I_1 is given by Middleton (25) to be

$$n(\hat{I}_1) = \sqrt{\frac{2}{\pi}} B \exp \left[-I_1^2 / 2I_0^2 \right] \quad (6)$$

where

B = Frequency spectrum width between half-power points (sec^{-1})

I_1 = Triggering level (amps)

I_0 = Root mean square noise = $(\hat{I}_1^2)^{1/2}$ (amps).

Equation (6) is applicable only to the type of noise specified and only for amplifiers that have a broadband Gaussian frequency distribution. To give a triggering level to rms noise ratio needed in limiting the spurious triggers to $n(\hat{I}_1)$ per second, the equation must be rearranged as follows:

$$I_1/I_0 = \left[2 \log_e \sqrt{\frac{2}{\pi}} B/n (\hat{I}_1) \right]^{1/2} \quad (7)$$

When the trigger level is set to discriminate against any signals that have an amplitude of less than \hat{I}_1 from the presence of an rms noise I_0 , the minimum signal-to-noise ratio at the phototube output necessary to initiate a reply is

$$\frac{I(t_p)}{I_0} = \left[2 \log_e \sqrt{\frac{2}{\pi}} B/n (\hat{I}_1) \right]^{1/2} \quad (8)$$

where t_p = time at signal peak.

Positive operation requires that the signal strength be somewhat above the triggering level, and a safety factor will be included to meet this requirement. A workable system then is one in which the peak signal-to-noise ratio will be at least N times the minimum necessary signal-to-noise ratio. This safety factor should be large enough to account for operation under most adverse atmospheric and sea state conditions and to discount any errors arising from the simplifications used here. Until an investigation of the zenith angle dependence of the signal strength has been deemed worthwhile, N must allow for some signal attenuation stemming from this variable. For daytime noise, the limiting equation for interrogator-to-transponder operation is derived from Eqs. (2), (4), and (8) in the following manner:

$$\frac{\int_0^\infty A_{mg}(\lambda) T(\lambda) S(\lambda) H_I(\lambda, t_p) d\lambda}{(2meI_D B)^{1/2}} \geq N \left[2 \log_e \sqrt{\frac{2}{\pi}} B/n (I_1) \right]^{1/2} \quad (9)$$

For nighttime noise, the limiting equation is obtained from Eqs. (2), (5), and (8) in the following manner:

$$\frac{\int_0^\infty A_{mg}(\lambda) T(\lambda) S(\lambda) H_I(\lambda, t_p) d\lambda}{(2meI_N B)^{1/2}} \geq N \left[2 \log_e \sqrt{\frac{2}{\pi}} B/n (I_1) \right]^{1/2} \quad (10)$$

Operation in the reverse direction, i.e., from transponder to responder, will be governed by two similar expressions. In this case it is not required to have a minimum signal-to-noise ratio as large as the one used in the previous case. Since an operator

is present to choose between signal and noise, a higher percentage of spurious triggers can be tolerated. Let this triggering rate be $m(I_1)$; then for daytime operation

$$\frac{\int_0^{\infty} A_{mg}(\lambda)T(\lambda)S(\lambda)H_T(\lambda, t_p)d\lambda}{(2meI_D B)^{1/2}} \geq N \left[2 \log_e \sqrt{\frac{2}{\pi}} B/m(I_1) \right]^{1/2} \quad (11)$$

and for nighttime operation

$$\frac{\int_0^{\infty} A_{mg}(\lambda)T(\lambda)S(\lambda)H_T(\lambda, t_p)d\lambda}{(2meI_N B)^{1/2}} \geq N \left[2 \log_e \sqrt{\frac{2}{\pi}} B/m(I_1) \right]^{1/2} \quad (12)$$

The conditions which must be fulfilled in order that day or night basic IFF systems may be declared workable appear in a quite general manner in Eqs. (9) through (12). They also allow for speculation on the many possible variations in system parameters that might be necessary to accomplish a feasible system. In order for an evaluation to be made of the existing experimental data, it is necessary that the equations be reduced to those covering more specific situations.

A reasonable upper limit to the aircraft search height of 600 meters will be assumed. The attenuation coefficient over this path length in air will be taken as $\alpha(\lambda) = 0.4$ kilometer⁻¹, i.e., a constant over the spectral region of interest. Dunkelmann (26) found quite wide variances of the atmospheric attenuation coefficient with wavelength at different localities. From his data we have selected an $\alpha(\lambda)$ value not unlike the one that might be expected as an average of the spectral values of this coefficient over sea water. In any case, the atmospheric attenuation will remain a minor factor at this height except when fog occurs. If these specific values of aircraft height and atmospheric attenuation are substituted in Eq. (1), the peak spectral irradiance at the transponder becomes

$$H_I(\lambda, t_p) = H_T(\lambda, t_p) = \frac{J_I(\lambda, t_p) \exp[-\beta(\lambda)r_s - 0.24]}{(r_s + 600)^2} \quad (13)$$

To complete the reduction of the general equations to more specific ones, the safety factor N is tentatively set at the comparatively large value of 25. Possible further reductions of this value will depend upon experimental evidence gathered in the future. It will also be required that the transponder spurious trigger rate $n(\hat{I}_1)$ be limited to one trigger a day. Similarly, the responder spurious trigger rate $m(\hat{I}_1)$ is taken as the same value for the present. This equivalence has been made until such time as an investigation determines the number of allowable spurious triggers when an operator is present. In either transponder or responder, the minimum signal-to-noise ratio for positive operation during day or night can be derived from Eqs. (9) or (11) by substituting in the foregoing values in the following manner:

$$N \left[2 \log_e \sqrt{\frac{2}{\pi}} B/n(I_1) \right]^{1/2} = 53.6(4.84 + \log_{10} B)^{1/2} \quad (14)$$

The unspecified factors remaining in Eqs. (9) through (12) are the parameters of the system and two variables, viz., sea water transmission and depth of the submarine transponder.

In the case of the present experimental equipment an analysis of each parameter will be carried out. Signal-to-noise ratios can then be formed as indicated by the left side of the limiting equations. Water transmission and other variables are employed that agree with the conditions under which shipboard data were obtained. Comparison of the results with experimental findings will show the reliability of the equations and the parameter measuring techniques. Extrapolation to an aircraft-submarine IFF system can then be made with confidence, and the complete limiting equations can be used to determine the conditions for which positive operation of the present equipment acting as an IFF system may be achieved. Further, with the accuracy of the measuring techniques and equations established, it will be possible to speculate on the easiest manner in which parameters may be changed in order to improve the system.

It is now quite impracticable to attempt an analysis of the parameters of the former equipment. A limited evaluation of this equipment, however, can be made by direct use of the experimental data.

During a nighttime shipboard run in May 1952, the experimental points on Curve A of Fig. 5 were measured using a band of ultraviolet wavelengths centered around 370 $m\mu$. Cable-length and leakage difficulties limited the measurements to a maximum depth of 200 feet. These data have been extrapolated to the point where the signal-to-noise ratio is estimated to be unity (2), and the result is Curve A. By an appropriate application of relations similar to those in Eq. (13), Curve A can be used to determine the signal-to-noise ratios which would have occurred if the receiver had been operated at an altitude of 600 meters instead of sea level and if the transmitter had been operated in sea water of any type.

The receiver bandwidth necessary to pass the 30-microsecond flash pulse was 33 kilocycles. Using Eq. (14), a minimum signal-to-noise ratio of 164 is obtained for reliable operation of the equipment as an IFF system.

A listing of the values assigned to the variables and a few of the parameters of the system used in calculating the curves of Fig. 5 follow.

$$r_a = 600 \text{ meters}$$

$$\alpha = 0.4 \text{ kilometer}^{-1}$$

$$\beta_A(370) = 0.074 \text{ meter}^{-1}$$

$$\beta_B(370) = 0.074 \text{ meter}^{-1}$$

$$\beta_I(370) = 0.04 \text{ meter}^{-1}$$

$$\beta_{II}(370) = 0.13 \text{ meter}^{-1}$$

$$\beta_{III}(370) = 0.26 \text{ meter}^{-1}$$

$$\beta_1(370) = 0.73 \text{ meter}^{-1}$$

$$N = 25$$

$$B = 33 \text{ kilocycles}$$

$$n(\hat{I}_1) = 1.157 \times 10^{-5} \text{ sec}^{-1}$$

$$m(\hat{I}_1) = 1.157 \times 10^{-5} \text{ sec}^{-1}$$

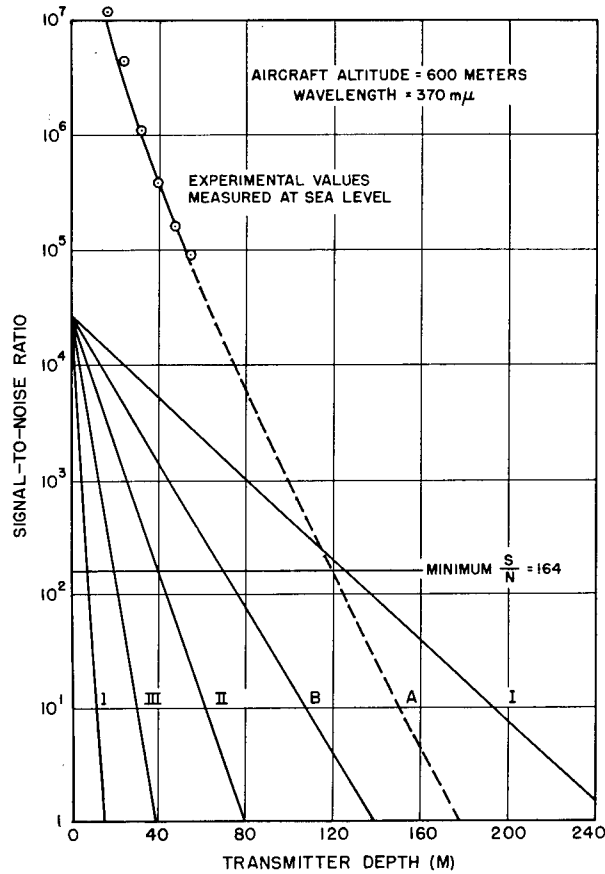


Fig. 5 - Nighttime operation of the first equipment acting as a transponder-responder section of an IFF system

Curves I, II, and III represent IFF operation in their respective types of ocean water. Curve B represents operation in ocean water of a type similar to that of Curve A. The importance of knowing the location of the boundaries of coastal waters is aptly illustrated by Curve 1 representing type (1) coastal water. Here, reliable operation of the equipment as an IFF system could be achieved only to a depth of seven meters.

This limited evaluation illustrates for one wavelength the manner in which shipboard experimental data can be used to determine the operating qualities of equipment acting as a submarine-to-aircraft identification system. A more complete evaluation of the experimental data is possible when the individual behavior of each system parameter is studied and related through the limiting equations to the signaling process as a whole.

EXPERIMENTAL TRANSMITTER

Previous field investigations had shown the need for a number of improvements in the transmitter. Its size and weight together with the added weight used in submerging were of such proportions that it was too unwieldy for safe shipboard use in any but the

calmest weather. At the cable depth limitation of 200 feet the water pressure was sufficient to cause leakage through the window seal. Power requirements necessitated the use of an excessively heavy cable which, for portable equipment, proved troublesome in handling. A desirable feature, from the standpoint of reception, was a variable self-flashing rate that ranged up to two flashes per second. For the type of flashtube used this rate was chiefly responsible for the excessive sizes and weights involved, since heavy-duty circuit components were needed to handle the power requirements. In addition to these objections there was room for considerable improvement in the signal characteristics of the flash.

Basically, a flash of this kind is derived from the sudden release of stored capacitor energy discharging through a tube usually containing an inert gas at a pressure which varies anywhere from millimeters of mercury to an atmosphere or more. Intense spark and flash discharges obtained in this manner are characterized by plasmas in which the degree of ionization is high. Further, the energy radiated by the plasma consists primarily of an intense continuum on which there is superimposed to some degree the characteristic line spectrum of the gas.

Certain features are desirable in a flash discharge to be used for signal work of the type described here. The most essential is the attainment of high peak intensity and short duration with as little electrical energy dissipation as possible. The reasons are obvious: longer ranges and higher flashing rates are obtained with smaller equipment, and a decrease occurs in the visual perception of the flash—a fact important when security is necessary.

It has been shown by Olsen and Huxford (27) and others that the peak spectral intensity of a flash varies approximately as the square of the peak-current value; the exponent is greater than two in the ultraviolet region and less than two in the infrared. Thus, it is advantageous for signal improvement to raise the current peak to as large a value as possible. For a given flashtube and amount of storage capacitance, this may be accomplished by minimizing the resistance and inductance of the discharge circuit.

The previously used flashtube, a General Electric FT-503, was designed primarily for studio photography where the maximum time-integrated, and not the peak, light intensity is the important factor. For this reason, the tubes are customarily used with a large capacitor (e.g. 200 microfarads) charged to a normal working voltage of four kilovolts. By combining a large amount of capacitance with a long path length for the discharge tube, a considerable integrated light output is obtained. In normal use the flash duration is of the order of a millisecond.

The FT-503 was selected for use simply because, of all the tubes readily available, the manufacturer's specifications for this tube quoted the highest peak intensity for a flash.

In order to convert the lamp from a photographically desirable one to one more suitable for signaling, it was necessary to depart from the usual values of the circuit elements associated with it. The energy (E) stored on a capacitor charged to a potential (v) is

$$E = \frac{1}{2} CV^2 \text{ joules} \quad (15)$$

where

C = Capacitance in farads

V = Potential in volts.

A small capacitor of 1.5 microfarads was chosen to reduce the physical size and self-inductance. Partial compensation for the loss in stored energy resulting from the change as determined by Eq. (15) was made by increasing the maximum operating voltage to 11 kilovolts. Above this operating potential there was a tendency for the discharge to fracture the quartz tubing. The net effect of the change was to maintain the high peak intensity while bringing the flash duration down to 30 microseconds. Limiting the signal improvement that may be accomplished in this fashion are the designs of tube, capacitor, and circuit. In this case, the lengthy flash-discharge path (50 cm) was concentrated by winding the quartz tubing into a spiral form. This helix adds greatly to the inductances of the capacitor and wiring already limiting the current peak.

Overvoltage breakdown for this tube occurs at about 5 kilovolts, a figure well below the desired operating potential. To operate at higher potentials, it was necessary to use a series holdoff switch. For this purpose a hydrogen thyatron was selected and worked satisfactorily. The thyatron was triggered to conduction simultaneously with the application of a triggering pulse to the flashtube.

In spite of the modifications, there remained a number of limitations associated with the FT-503 and its circuitry. The inductance of the spiral design of the tube, the resistance of its long low-pressure path length, and additional inductance and resistance due to the need of a switch-acting thyatron leads to values of the peak current that are much lower than could be achieved with a properly designed flashtube. A capacitor of the ordinary power-service type was used as the discharge capacitor. In the construction of these capacitors little attention is paid to self-impedance characteristics. Triggering to conduction is accomplished by means of a spark coil applied to a wire wound around the flashtube. This external triggering not only requires excessively high potentials but is also quite erratic. Owing to the spiral flashtube design, the heavy current pulses apparently stress the tubing unduly, and as a result, an additional limitation is placed on the peak-current value. Finally, the pressure of the gas filling and the path length are not those that should be selected for best signal characteristics.

When plans for a new transmitter were commenced, a rather complete search was made among the commercially available flashtubes for one embodying the most desirable features for this work. Although a majority of the high-intensity commercial tubes are made from the standpoint of flash photography, some are designed for short-duration exposures. In particular, a British tube, the Mullard LSD2 microsecond flashtube (Fig. 6), combines both short duration and high intensity by using a fairly short gap with a high-pressure filling (approximately 1 atmosphere of argon plus 5 percent of hydrogen). The tube is rated to hold off potentials up to 11.6 kilovolts and is easily triggered to conduction by means of an internal trigger electrode. In actual operation it broke down intermittently at voltages above 6 kv.

If an IFF system should eventually prove feasible, it is unlikely that any flashtube of present commercial design could be used as an adequate signal source. This would be especially true for a communication system using high repetitive rates. From the present experimental standpoint, however, the prime interest is in obtaining data from which the determination of the feasibility of an IFF system may be made. Considering this it may be justifiable to use an excessive amount of energy in the attainment of high

peak intensities for experimental work. This would not necessarily be the case in operational gear. Research on the design of a tube suitable for operational use is also being conducted by the authors. These investigations, however, will be considered separately, and no further mention of this work will be made here.

The transmitter has conventional flashtube charge and discharge circuits (Fig. 7), and proper emphasis is placed on the lead and component location in the discharge circuit in order to minimize the self-inductance. High peak currents are obtained because of the short straight discharge path of the tube and by operation below the breakdown voltage which eliminates the need of a switch tube. To reduce the size of components, a slow flashing rate of one every five seconds was decided upon, and to further conserve tank space, the triggering was manually controlled from the surface. The triggering rate of the previous transmitter was controlled by a relaxation oscillator and associated circuitry in the tank. A compactly packaged high-voltage supply having an output continuously variable from 0 to 12 kv is used and is capable of delivering a rated maximum current of 1.5 ma. The input to the supply is Variac-controlled through the power cable from the shipboard controls. A Sprague type Y51216 special capacitor is employed as the energy storage element, and its 0.5-microfarad value is a compromise between energy storage and physical size. The charging time of the storage capacitor (time to reach 95 percent of maximum voltage) is five seconds. Special features of this capacitor are its low internal resistance and inductance values. Triggering the flashtube is accomplished by discharging a 0.25 μ fd capacitor with a relay into the primary of a trigger transformer whose secondary is connected to the internal trigger electrode of the flashtube.



Fig. 6 - Mullard LSD2 flashtube

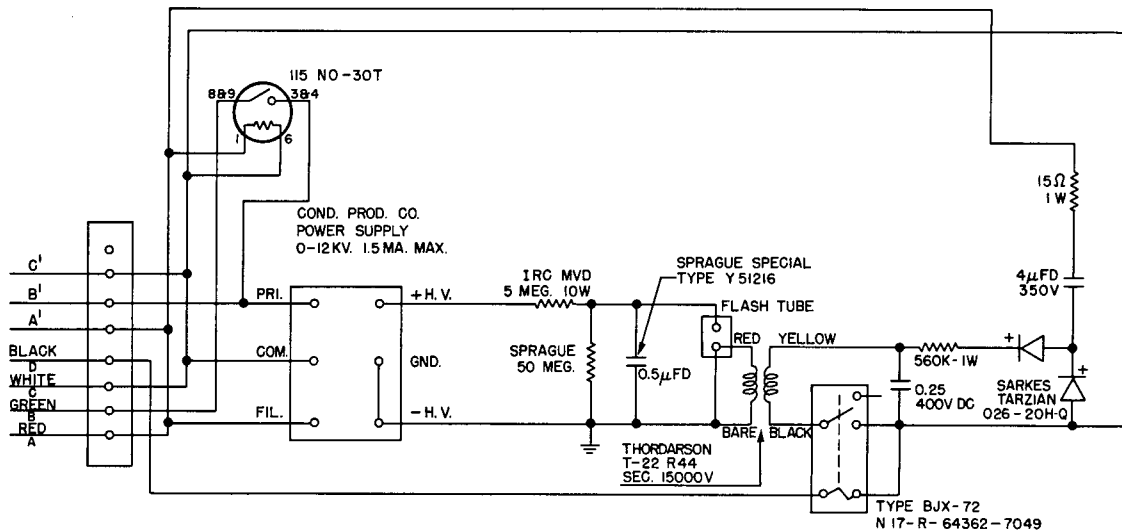


Fig. 7 - Schematic diagram of transmitter charge, discharge, and trigger circuits

The oscillographic photographs shown in Fig. 8 illustrate the characteristics of the discharge; Fig. 8a shows the oscillatory nature of the discharge current. For reasons of simplicity, the time derivative of the current rather than the current itself was obtained because attainment of this function was easily accomplished by measuring the voltage induced magnetically in a pickup loop placed adjacent to the discharge circuit. A good estimate of the peak current can be obtained from the usual relations for an underdamped LC circuit. The peak discharge current I is given by

$$I = V \sqrt{C/L} \text{ amps} \quad (16)$$

where

C = Discharge capacitance (farads)

V = Potential on capacitor (volts)

L = Inductance of the discharge circuit (henrys).

Now V and C are known in this case, and it remains only to determine the inductance L . From the frequency relation for an oscillatory circuit,

$$f = \frac{1}{2\pi} \sqrt{1/LC}, \quad (17)$$

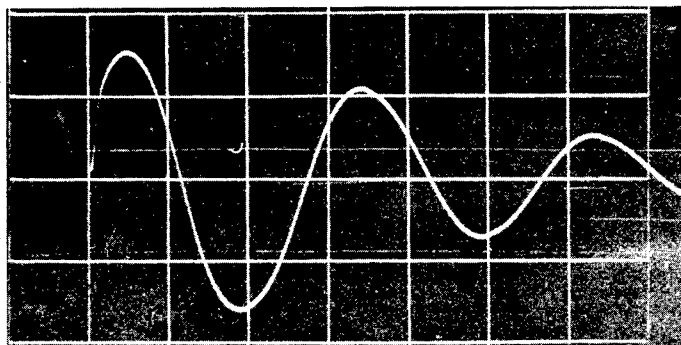
and using a frequency of 330 kilocycles as determined from Fig. 8a, a value of L equal to 0.4 microhenry is obtained. Substituting this into Eq. (16) it is apparent that the peak current is approximately equal to 1.1 times the magnitude of the charging potential. For example, if the potential V were six kilovolts, the resulting peak current during the discharge would be about 6600 amperes. The peak current for the former transmitter was measured as 1500 amperes for the same potential.

Light output as a function of time was measured simply with a 935 phototube (Fig. 8b). The pulse width at half-peak intensity is 1.4 microseconds, but a considerable tail-off to the pulse remains as a result of the succeeding current peaks and decay of metastable states.

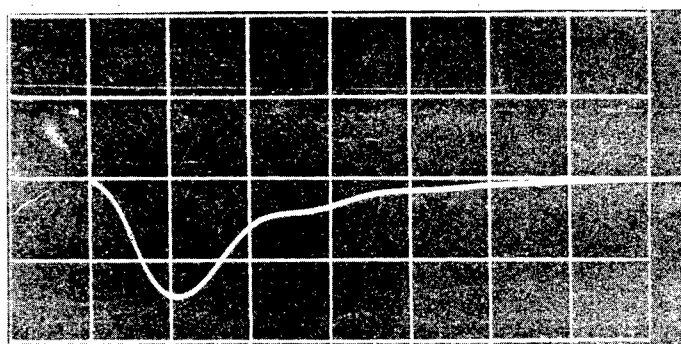
The peak spectral intensity distribution of the flash was investigated for a discharge potential of 6 kv (Fig. 9). Measurements were made with a Gaertner quartz monochromator and a photomultiplier tube and were corrected by the use of a standard color temperature lamp. Since standard pulse techniques were used and all methods were conventional, no further elaboration is needed.

The measured area of the curve, between the wavelengths of 300 and 680 $m\mu$, gives a value of 2.04×10^4 watts/steradian for the peak radiant intensity, and 2.57×10^5 watts for the peak radiant flux.

The limited number of measurements made in obtaining the curve were sufficient to give only a rough outline of the intensity distribution and quite insufficient to resolve any spectral lines. The more prominent peaks, however, agree in wavelength with groupings of intense argon spark lines. Poor resolution would produce values of intensity and flux that are somewhat in error. The actual values of these quantities may be somewhat lower



(a) Time derivative of the discharge current



(b) Time function of the light output

Fig. 8 - Characteristics of the LSD2 flashtube and discharge circuit. The sweep time is 1 cm per microsecond

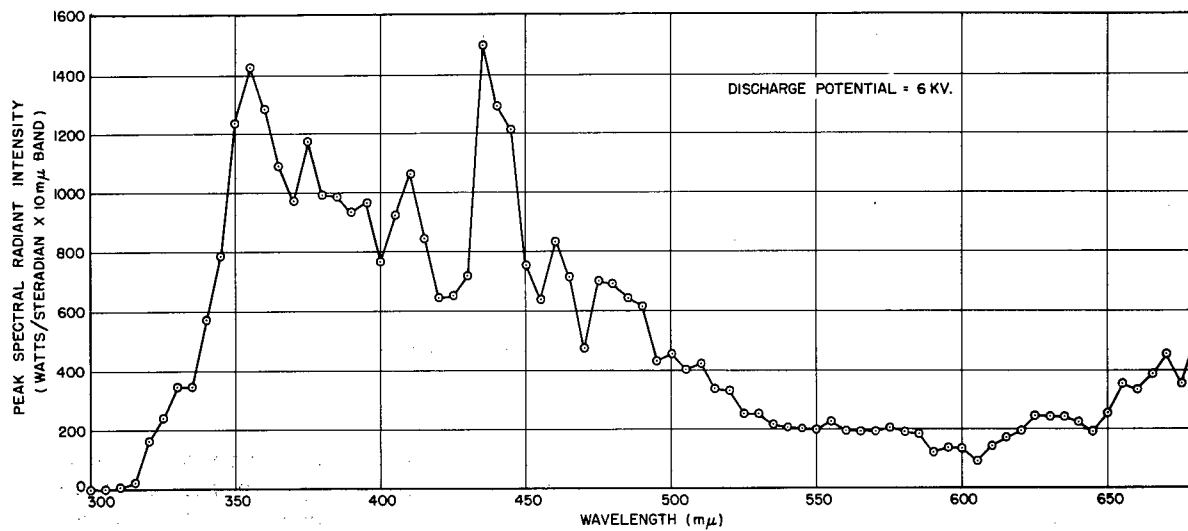


Fig. 9 - Peak spectral radiant intensity of the LSD2 flash

than quoted. In addition there is another, somewhat smaller, error in these quantities. Let the spectral radiant intensity distribution at a given time be pictured as a thin slice of a three-dimensional mountain range. The intensity values start from zero at all wavelengths at zero time, rise to maxima, and fall away again eventually to zero. The peak intensity is known experimentally to occur at a slightly later time in the red spectral region than in the ultraviolet (27). The curve of Fig. 9 represents simply the measured peak values at all wavelengths. An actual measurement of the radiant intensity or flux at a given instant would result in values lower than those obtained from such a curve. In the use of the curve in this work only peak intensity values for narrow bands of wavelengths are needed, and as a result, the time-difference error is negligible.

A maximum operating depth of 500 feet was planned for the new transmitter (Fig. 10). With 220 psi pressure present at this depth, the 1/4-inch mild-steel casing has an estimated safety factor (28) of three over the collapsing pressure. Window and casing seals are of the static O-ring type, and O-rings are also used as packing in the watertight cable pass-through. In the previous transmitter, fused quartz was used for the window because of its excellent ultraviolet characteristics. However, it had a tendency to chip while being drawn tight in the sealing process, and as a result, satisfactory service was largely dependent on caution in handling. Pyrex was investigated as a substitute and eventually used. Its ultraviolet properties (Fig. 11) are sufficiently good to rule out the expense of using quartz.

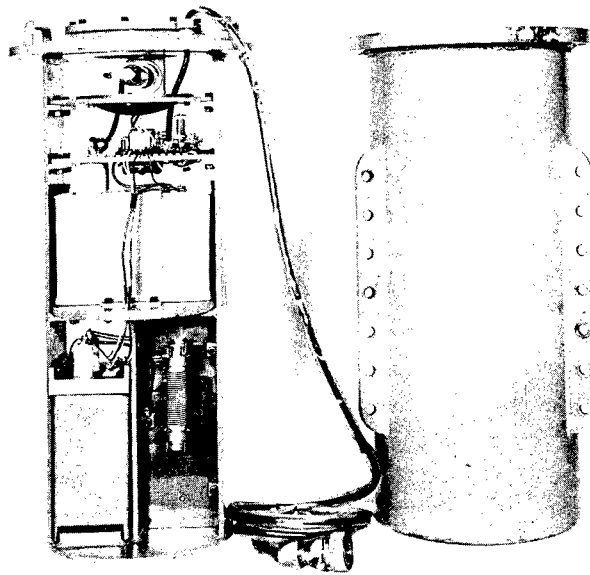


Fig. 10 - Transmitter unit and watertight casing

To determine the resistance of pyrex to possible fracture from pressure, a 3/8-inch window was tested to destruction in a water pressure tank. Shattering occurred at approximately 400 psi, and for an additional margin of safety, the final windows were made one-half inch thick. For a complete check of all seals, the transmitter was subjected to a pressure of 250 psi (equivalent to a water depth of 560 feet) for two hours during which no leakage occurred.

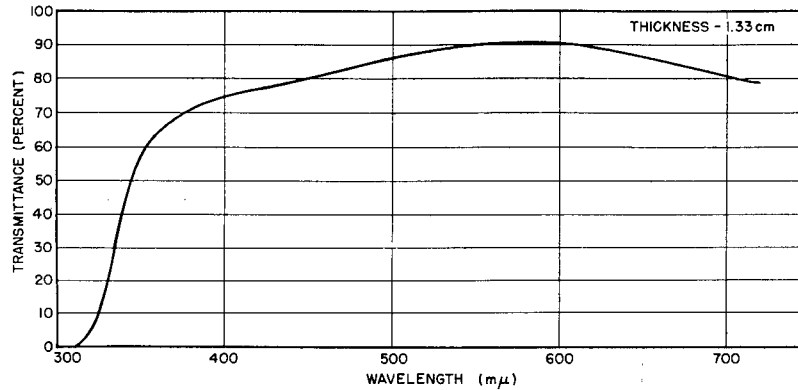


Fig. 11 - Transmittance of pyrex window used in transmitter

The completed transmitter weighs 175 pounds. Power requirements are quite low, thus permitting the use of a small 5/16-inch-diameter four-conductor power cable. Although not designed for underwater use the cable worked well. Precautions were taken to assure that its thin rubber coating received no rough treatment. For convenience, a quick-disconnect Royn cable connector permitted separation of transmitter and power cable. The cable storage reel was provided with slip rings to permit continuous operation, and this feature gave considerable improvement over the previous operation.

An aluminized, spherical, metal mirror was used in the transmitter to provide enhancement of the signal flux, and the gain factor thus obtained is about 2.5 for most of the visible spectrum (Fig. 12). It seemed unjustifiable to attempt to bring about much increase in the signal-to-noise ratio by optical methods in the experimental equipment which must descend to the depths attained by submarines. The window apertures needed for appreciable gains would add greatly to the equipment problems and also add further to the window shattering problem.

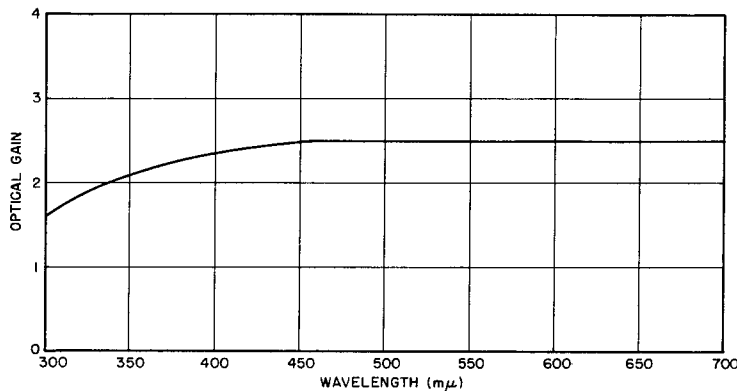


Fig. 12 - Spectral gain obtained by using a mirror in the transmitter

In using the peak spectral radiant intensity of the LSD2 flash (Fig. 9) to calculate signal irradiance, it is necessary to correct for the pyrex window transmission and the optical gain factor. When this has been done, the result will be an equivalent beam spectral radiant intensity, $J_I(\lambda, t)$, as used in Eq. (1).

EXPERIMENTAL RECEIVER

The discussion of the receiver may best be begun by referring to the limiting equations for interrogator-to-transponder operation (Eqs. 9 and 10) and the complementary equations for transponder-to-responder operation (Eqs. 11 and 12). The receiver parameters which affect the signal-to-noise ratios as defined in these equations are as follows:

$S(\lambda)$ = Spectral sensitivity of the photosensitive device

$T(\lambda)$ = Transmission of optical filters used with the receiver

$g(\lambda)$ = Gain of the receiver optics

A = Area of the photocathode

m = Current amplification (when using a photomultiplier tube)

B = Electronic bandwidth of the receiver.

Rodda (22) showed that when the noise limit of the receiver is determined by the dark current I_N of the phototube a substantial increase in signal-to-noise is possible through the use of a photomultiplier in place of a phototube. Such a case will occur under ideal night conditions, and this is the reason for choosing the photomultiplier in the receiver design.

The daytime equations are complicated by the behavior of the average anode direct current I_D which is a function of background illumination. The approximate dependence of I_D is easily determined as

$$I_D = \frac{\omega}{\pi} \int_0^{\infty} T(\lambda) S(\lambda) W(\lambda) m A d\lambda \quad (18)$$

where

ω = Solid angle of the field of view (steradians)

$W(\lambda)$ = Average radiant emittance in the field of view (watts/meter²).

If an optical rather than a collimation system is employed, the factor ω/π may be replaced by $1/4F^2$, where F is the F -number of the optical system. Either F or ω is considered as an additional parameter of a particular receiver system.

Combining Eq. (18) with either Eqs. (9) or (11) shows that in daytime the S/N ratio is independent of the current amplification m . That the result should be independent of m is expected, since all photocurrents will be amplified alike.

To prevent fatigue in any photosensitive device, the average anode current must be limited to some safe maximum value. Equation (18) shows that although I_D must be held to a fixed limit, there are any number of possible variations in the system parameters permissible while still accomplishing this. The nighttime S/N ratio may be improved by increasing the values of most of the parameters. However, in daytime with I_D restricted to a maximum safe amount, it is necessary to lower parameter values in order to accomplish this decrease. Improvement in daytime S/N ratio at the receiver is achieved mainly through collimation, or increasing the F/number and optical gain. For a combination day-night receiver using collimation, the best multiplier tube should have a large area, and therefore the RCA 5819 end-on tube was selected.

Bidirectional daylight measurements were contemplated with the equipment. The necessity then of encasing the receiver in a watertight housing precluded the use of any optical gain in the experimental equipment. The rated average maximum anode current of the 5819, according to the manufacturer's specifications, is 100 microamperes. It was decided not to exceed 5 microamperes in the present case since the tube must operate indefinitely at this level. Such a value, which is certain to be reached under daylight operation, placed considerable restrictions on the receiver parameters. Future experimentation may show this value to be low even for continuous operation, although the improvement in S/N ratio gained by raising it will be small since the daylight S/N is independent of m .

To restrict the anode current to 5 microamperes under the expected average daylight conditions, it was experimentally found necessary to reduce considerably the amount of radiation incident on the bare photomultiplier at a current amplification of unity. For this purpose, collimation and narrow-band interference filters were used. The collimation to a solid angle of 0.5 steradian served a two-fold purpose, i.e., it reduced the amount of incident light on the photocathode and prevented large angles of incidence on the interference filters. The bandwidth of the interference filters increases as the sine of the incident angle increases.

An entire receiver with the exception of the watertight casing is shown in Fig. 13. A Baird interference filter and an ordinary companion filter are seen in the foreground. The 5819 tube on the right is provided with a mu-metal shield which can be seen at the end of the electronics section. The whole is in turn encased in the light-tight housing which provides the collimation and mounting for the filters.

Separate investigations of each parameter of the receiver were conducted. The spectral sensitivity and current amplification of a particular tube are shown in Figs. 14 and 15. Current amplification as a function of phototube voltage was determined by the use of calibrated neutral filters and a light source. Beyond 600 volts amplification measurements were discontinued because of the dark-current noise limitation. The spectral sensitivity of the 5819 tube in absolute units was found by comparison with the calibrated 935 phototube mentioned previously.

There is an optimum bandwidth B for maximum signal-to-noise ratio if all other factors remain the same. This is not evident from Eqs. (9) through (12) where decreasing the bandwidth continues to give increased signal-to-noise ratio. The reason is that the bandwidth effect on the pulse signal has been neglected. Near optimum bandwidth conditions were assumed to exist in the development of the limiting equations. Thus, in order that these equations may be applicable it is necessary that this optimum bandwidth B be found and incorporated into the electronics of the receiver.



FIG 13

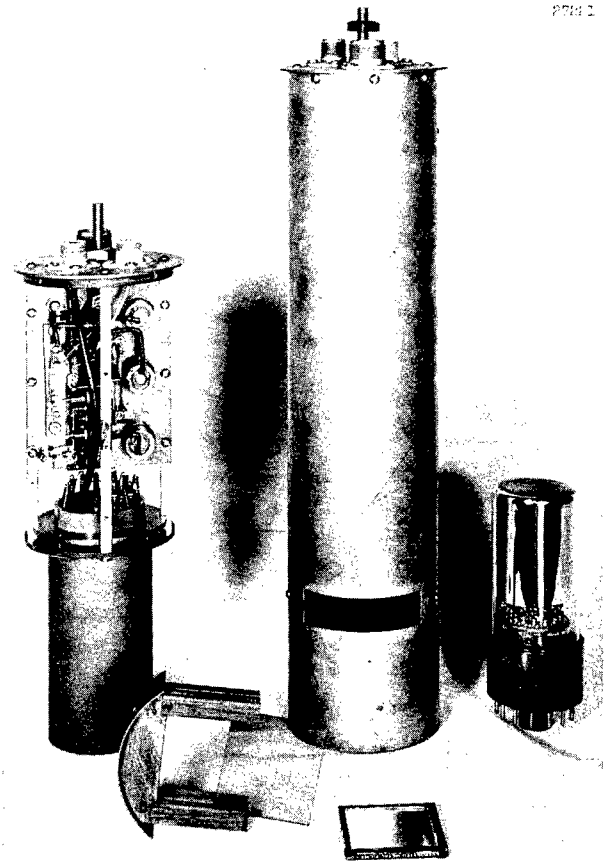


Fig. 13 - Receiver components



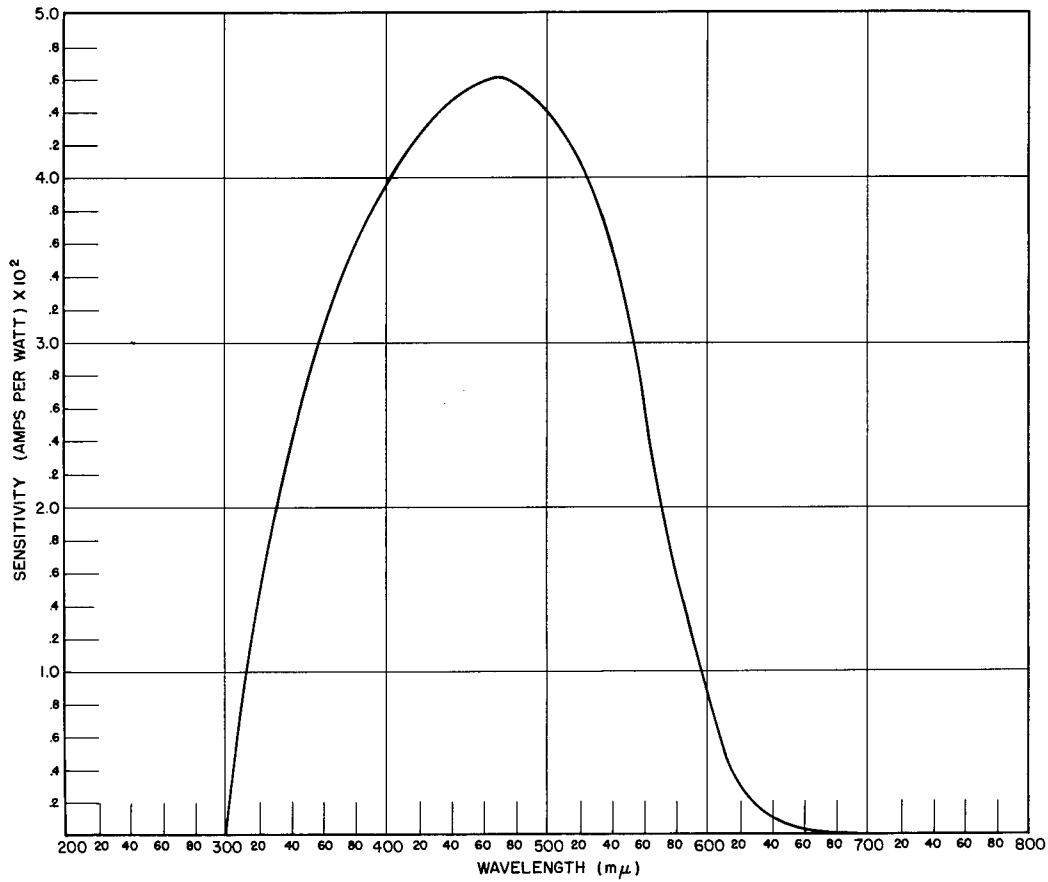


Fig. 14 - Spectral sensitivity of 5819 photomultiplier No. 5 at a current amplification of unity

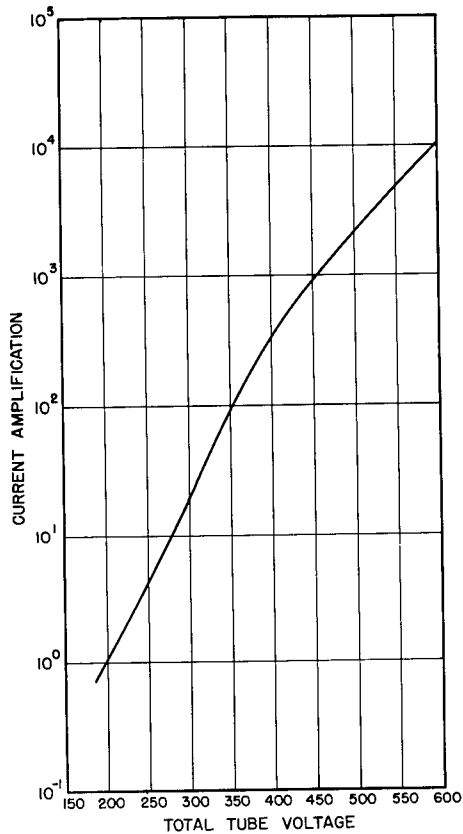


Fig. 15 - Current amplification of 5819 photomultiplier No. 5

For the rectangular pulses of radar work, a video bandwidth of $3/4 \times (1/T)$, where T is the pulse duration, is optimum. A good demonstration of this is a series of illustrations by Goldman (page 99 of Ref. 29). Any attempt to find the optimum bandwidth exactly for gas discharges runs into mathematical difficulties. The functional expressions for the light intensity are not the simple square pulses of radar, but are a great deal more complicated. Huxford et al. (30) are attempting to optimize the bandwidth for certain photocell receivers with an analytic expression suitable as an approximation to some gas discharges. However, this expression, which is of the form

$$K \left(1 - e^{-\frac{t}{T_1}} \right) e^{-\frac{t}{T_1}}$$

is not well-suited to the flash pulse as obtained from the transmitter described here. Rather the function

$$At^2 e^{-a^2 t^2}$$

has been found to be a closer approximation; the agreement between it and an actual flash pulse over most of the flash duration is illustrated in Fig. 16. If the tail-off of the approximating pulse is presumed to represent the decay of metastable states, the slower tail-off of the true pulse could possibly be due to succeeding peaks of the damped sinusoidal current. It is curious that this particular function should represent so closely the flash pulse since it is similar to the Maxwell distribution function. Whether this is a coincidence may well bear investigating on other flash discharges.

The mathematical solution for optimum video bandwidth through the use of the analytic pulse expression has not been attempted. Instead a semiempirical method was employed whereby the frequency spectrum of the pulse was found and the amplifier's response curve tailored to suit it. To find the frequency spectrum of the pulse, it is necessary only to find the absolute value of its Fourier transform. The resulting spectrum for the pulse in question is shown in Fig. 17 along with the frequency-response curve of the amplifier. Response of the amplifier was tailored by adjusting the values of circuit constants. At the upper and lower limits the half-power points were set to include the majority of frequencies in the pulse frequency spectrum. That the majority of frequencies at the lower end is included is not readily apparent from the figure because of the logarithmic plot.

In somewhat similar systems, Goldstein (23) demonstrated the presence of low-frequency noise (up to a few hundred cycles per second) resulting from the glitter of sunlight on the surface of water. To eliminate this as a noise source, the low-frequency response was deliberately suppressed. It was not necessary to cut off the low frequencies at as high a value as shown in the figure; however, noise generated in slip-ring contacts supplying the receiver voltages through a cable reel necessitated the selection of the higher value.

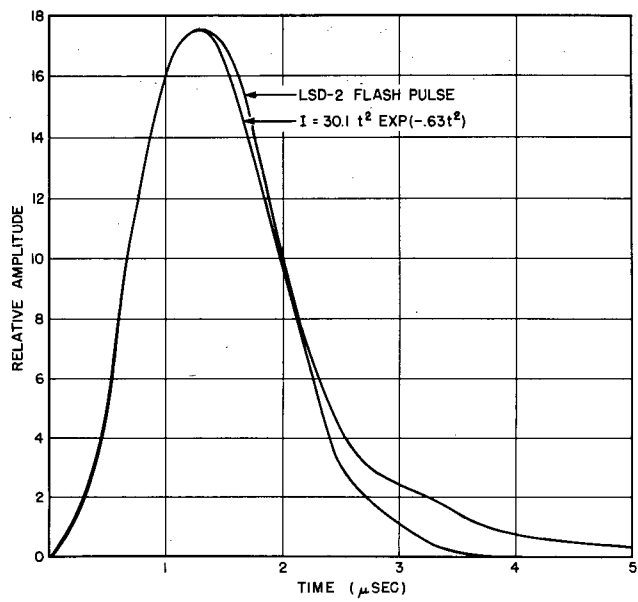


Fig. 16 - Comparison of actual flash pulse and approximating function

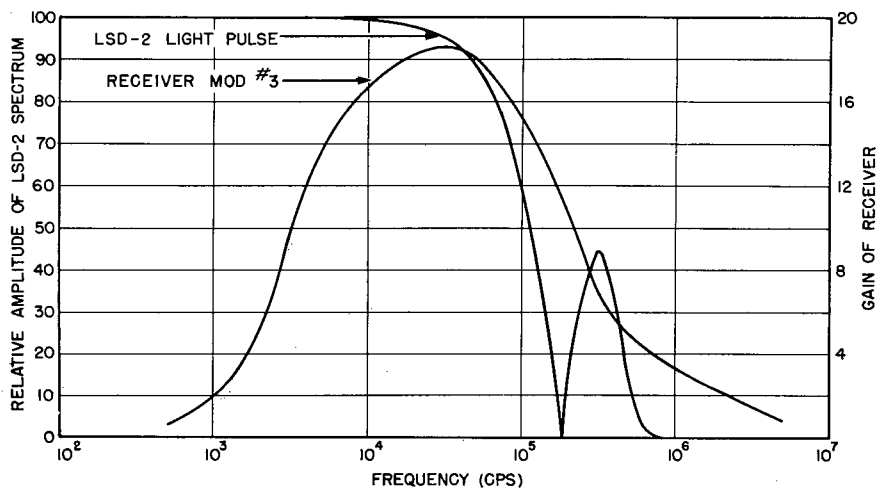


Fig. 17 - Frequency analysis of LSD2 pulse and frequency response of receiver

In addition to the optimum condition imposed on the bandwidth in the development of Eqs. (9) through (12), a further restriction is placed upon it in connection with Eq. (6). Validity of this equation depends on the bandwidth being broadband with a Gaussian distribution (22). Roughly this condition is satisfied by the amplifier response.

The video bandwidth, as determined from the area of a linear plot of the frequency vs. power gain of the amplifier, is 212 kilocycles. Stray and interelectrode capacitance in the input circuit would modify the measured bandwidth value slightly depending on the time constant of this capacitance and the photomultiplier anode resistance. A value of this resistance was chosen so that no lower value would visually improve the pulse display on an oscilloscope; as a result, little error could appear in the 212-kc bandwidth figure.

In the schematic diagram of the receiver (Fig. 18), a single stage of amplification is used with a cathode follower output. As much as 300 feet of coaxial cable is fed by the circuit when the receiver is submerged.

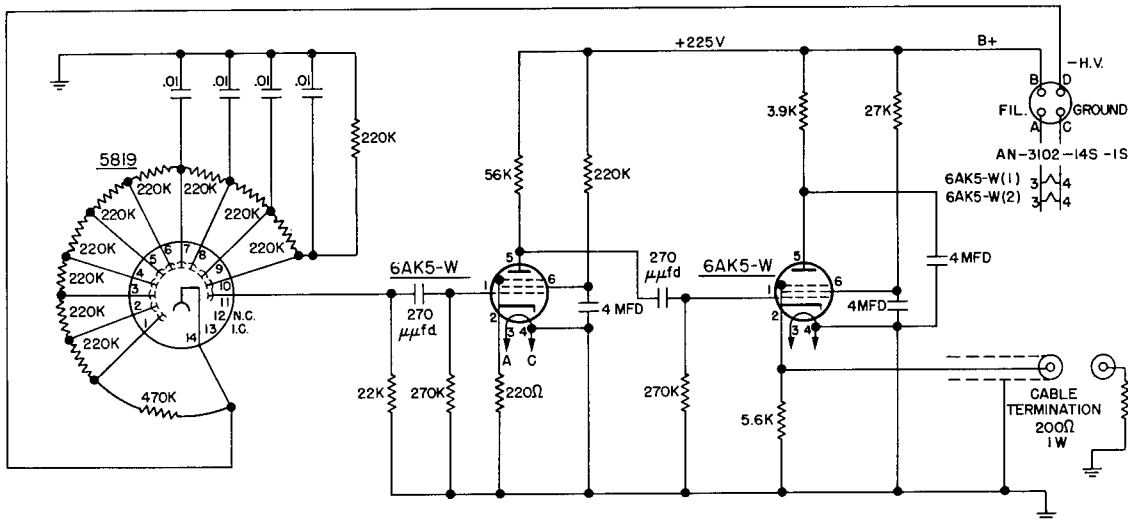


Fig. 18 - Schematic diagram of flash pulse receiver

A depth of submergence equivalent to only half that of the transmitter was planned for the receiver because of additional cable problems. Measurements down to this depth were intended to check the relationship between signal transmission in either direction, and more complete data taken with the transmitter submerged were then sufficient for use in both directions.

Signal pulses from the transmitter, as observed by the receiver, were displayed on a Tektronix 514D oscilloscope, and measurements were made on the peak values thus occurring.

An inconvenience in the experimental procedure and a complication of the receiver circuits would follow any attempt to measure directly the sunlight noise present during experimental operations. As an alternative a simple method was evolved, evaluated, and successfully used for this purpose.

It is noted, first of all, that for pure Gaussian noise Middleton's expression (Eq. 6) is a relationship between the rms noise and the number of noise triggers above a pre-determined value. Thus, with the trigger level of the oscilloscope fixed, the number of spurious triggers in a given time interval is a measure of the rms noise. Further, the rms noise is related to the anode current of the photomultiplier tube through Eq. (4). It was possible to measure in the laboratory the rms noise with five microamperes in the anode resistor and at the same time note the number of spurious triggers that occurred on the oscilloscope during one minute. With this knowledge it was possible to vary the current amplification (m) in the experiments at sea so that approximately the same number of triggers per minute would be obtained and five microamperes of current would be assured as a result of sunlight.

RESULTS

The experimental results were obtained while operating from the deck of the E-PCE(R) 851, which was enroute from NRL to Panama City, Florida. Only three series of measurements were taken because of the limited time available. For two of these the transmitter was lowered by a hoist and the receiver was mounted outboard on a boom. In the third series the reverse procedure was followed with the receiver being lowered. The remainder of the equipment associated with the measurement, i.e., the power supplies, controls, and oscilloscope, was mounted in the ship's experimental electronic compartment from where the measurements were made.

On a day with overcast skies, the first series of measurements were taken at a site located between the Gulf Stream and the Sargasso Sea. Figure 19 shows these measurements, and point (d) of Table 1 gives the exact location with its sea water classification. The solid curve represents the experimental S/N ratios measured at the various depths. Each point is the average of two or three values, and pulse heights at each depth duplicate themselves reasonably well. Signal-to-noise ratios were formed from the pulse-height data and also from the measured value of system noise when five microamperes of current were present in the anode circuit of the photomultiplier. Rounding off of the curve at shallow depths was due to signal saturation of the receiver amplifier.

An interference filter with a transmission band centered at $474 \text{ m}\mu$ was used in the receiver (Fig. 20). It was expected from rough calculations that maximum S/N ratios would be found near this spectral region. Through an oversight, two other transmission bands of the filter—one in the red region and one in the ultraviolet—were not excluded. Calculations, however, showed that they contributed negligibly to the signal and but slightly to the noise.

An average attenuation coefficient of $\beta(474) = 0.055 \text{ m}^{-1}$ was found by using the experimental results below the amplifier saturation point. This value, in terms of transmission per meter, agrees exactly with Jerlov's Type II ocean water at that wavelength and, because of the location, lends credence to his classification.

To check the agreement of the experimental data with the functional form of the S/N expression, a calculation of relative S/N ratios was made at various depths by using the previously mentioned value of $\beta(474)$. The values were adjusted to agree with the experimental curve at the 80-meter point, and the result is shown by the dashed curve of Fig. 19. Validity of the functional form of the expression is believed to be justified by the overlap of the two curves in the region where the amplifier response is linear. Agreement at shallow depths was indicated by Fig. 5.

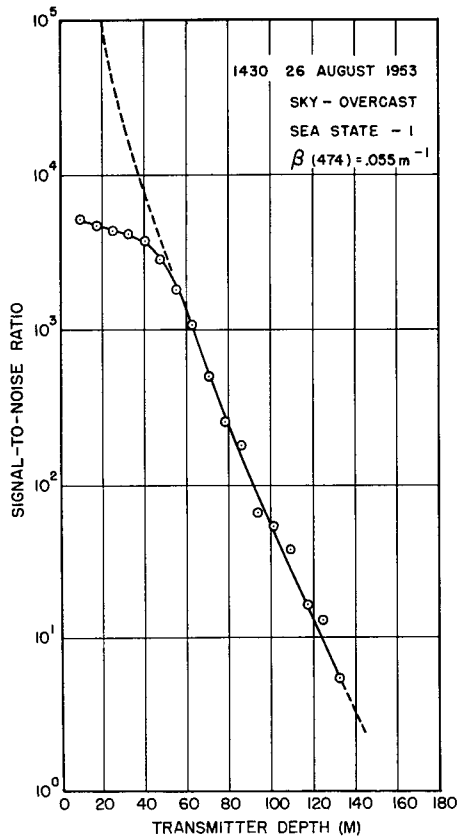


Fig. 19 - Measurement series No. 1; the solid curve represents the measured values and the dashed curve the calculated results

The validity of the expressions (Eqs. 9 through 12) for determining the absolute values of S/N ratios depends upon their ability to give these ratios from measured values of all parameters of the system to an error well within the safety factor (N).

On this particular day, with the sun obscured, the flash of the transmitter was visible to observers at the ship's rail down to a depth of 75 feet. A transmitter depth of 432 feet was reached before noise interfered enough to prevent further measurements.

The second series of measurements was taken in the Gulf Stream on a clear day with the sun at a high altitude (Fig. 21). An attenuation coefficient of $\beta(474) = 0.066\text{m}^{-1}$ determined for this water puts it slightly below the Type II classification into which Gulf Stream water falls. The proximity to the coastline (nine miles) might well be the reason. As before, relative S/N ratios calculated by using a freeboard height of 4.5 meters were adjusted to agree with the experimental curve at the 80-meter point.

A transmitter depth of 382 feet was reached before noise interfered. The depth attained, which was less than in the first series, is explained by the higher attenuation coefficient of the water and an increased background illumination from the direct sunlight. The glitter of the sunlight on the water prevented the transmitter flash from being seen much below 32 feet.

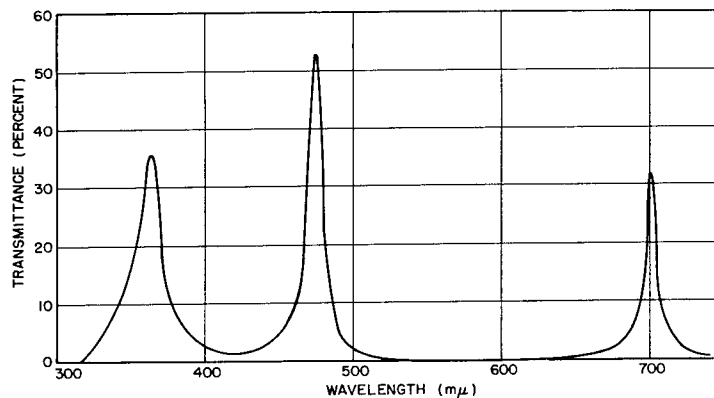


Fig. 20 - Transmittance of Baird interference filter No. 7-2781-B

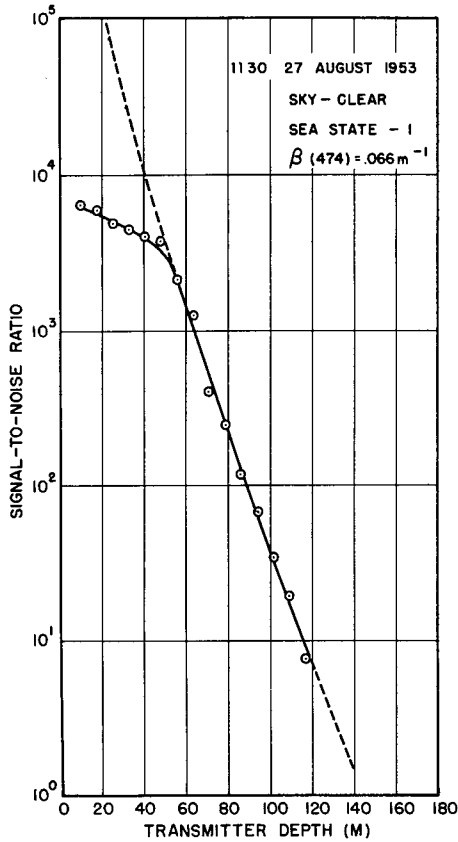


Fig. 21 - Measurement series No. 2

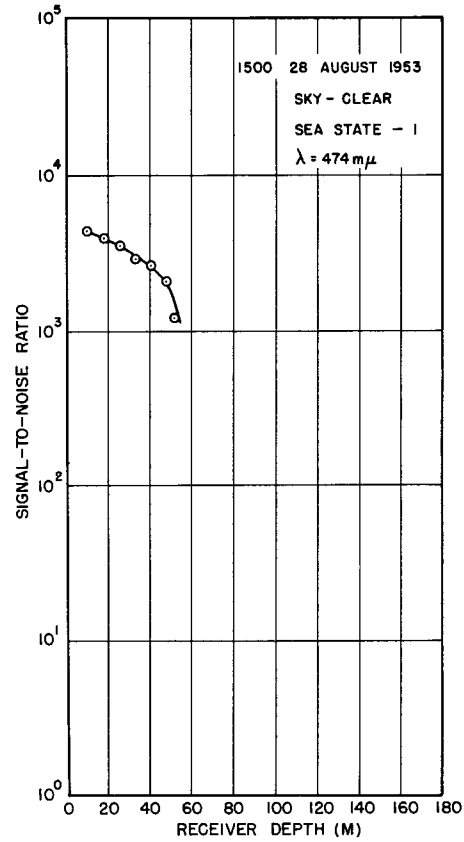


Fig. 22 - Measurement series No. 3

Since an IFF system requires two-way transmission and reception, it was considered necessary to obtain experimental data with a submerged receiver. There is no reason for believing that the nighttime operation of the system would not be identical in either direction. But in the daytime it is apparent that the distribution and magnitude of the background radiance would differ in each case. The experimental data of Fig. 22 were taken in the Gulf of Mexico on an early afternoon with a clear sky. The flow of ocean current past the ship caused a considerable strain on the small-diameter coaxial signal cable and necessitated an extra amount of slack in it and the power cable. Sufficient depths to reach the linear range of the amplifier were not attained, and calculation of the attenuation coefficient was therefore not possible.

It may be well to point out that the electrical cables should have been clipped to the strain cable at regular intervals in order to prevent any large accumulation of forces on them.

Some information of value, however, was obtained from the results. First of all, the anode direct current of the photomultiplier, due to sunlight, did not exceed the 5-microampere current limit set for operation in the reverse direction. If a zenith sun were present, some current increase might be expected at shallow depths. Second, the anode current might be expected to decrease as the receiver depth increases, and it did. The decrease was only slight at 160 feet, the greatest depth attained, where it was found possible to increase the current amplification (m) from a value of 1.0 to 1.8. Lastly, the

two measured S/N ratios on the curve, which are near the region of amplifier linearity, are not over a factor of two smaller than the corresponding measured data in the reverse direction. From these pieces of information it is concluded that the interrogator-to-transponder section of an IFF system will work equally as well as the transponder-to-responder section. This statement should hold at any wavelength since the measurements were made in the region of maximum sunlight penetration.

The limiting Eqs. (9 through 12) were derived for use in determining from calculations the feasibility of an IFF system under any given set of conditions. With the functional form of the S/N expressions confirmed, it remains to be determined whether they will give the correct ratios from measured values of all parameters. Calculations were performed for this purpose using the specific conditions of the first and second measurement series at an 80-meter depth. The following are the values assigned to the variables.

<u>Variable</u>	<u>Series 1</u>	<u>Series 2</u>
r_a	4.5 m	4.5 m
$\alpha(\lambda)$	0.4 km ⁻¹	0.4 km ⁻¹
r_s	80 m	80 m
$\beta(\lambda)$	Fig. 3 assigning $\beta(474) = 0.055 \text{ m}^{-1}$	Fig. 3 assigning $\beta(474) = 0.066 \text{ m}^{-1}$
I_D	5 μa	5 μa

The attenuation in air is, of course, negligible. Variation of $\beta(\lambda)$ with wavelength over the transmitting region of the interference filter is from Jerlov's data. The value of I_D is taken as the experimental value only because no measurements were performed on the sunlight irradiance. A summary of the parameter values used in each case is as follows.

<u>Parameter</u>	<u>Series 1</u>	<u>Series 2</u>
A	$1.14 \times 10^{-3} \text{ m}$	$1.14 \times 10^{-3} \text{ m}$
m	1.0	0.73
B	212 kc	212 kc
$g(\lambda)$	1	1
$S(\lambda)$	Fig. 14	Fig. 14
$T(\lambda)$	Fig. 20	Fig. 20
$J_T(\lambda, t_p)$	Fig. 9	Fig. 9
Pyrex window	Fig. 11	Fig. 11
Mirror gain	1	Fig. 12

Integration of the signal expression to obtain the pulse height was performed by summing the necessary products over 5-m μ bandwidths. Forming the S/N ratios from noise values calculated from Eq. (4) gave the following results for comparison with the experimental values.

<u>Measurement Series</u>	<u>Exp. S/N</u>	<u>Calc. S/N</u>
1	2.6×10^2	0.74×10^2
2	2.2×10^2	0.78×10^2

The quotient of the experimental and calculated values is taken as a measure of the errors involved in the assumptions and in the parameter measuring techniques. The error in both series is well within the safety factor, and a sufficient amount of the safety factor is left for adverse weather conditions.

There is justification now to use the equations in finding a workable IFF system. To this end, a study of the performance of the equipment acting as a transponder-responder section of an IFF system will first be made in different types of sea water at a wavelength of 474 m μ . Pointed out previously is the fact that the interrogator-transponder section would operate equally as well. The calculated results for an aircraft at 600 meters and a submarine at variable depths are shown in Fig. 23. Equivalent sunlight conditions of Series 2 measurements are assumed to prevail, i.e., $\rho_m = 0.73$ and $I_D = 5$ microamperes. The background radiance is possibly near its maximum under these conditions. It is apparent from the figure that a workable IFF system is not possible in any sea water type during daylight at this wavelength. For the present, positive operation at a transponder depth of 50 meters will be taken as a determination of the feasibility. An increased factor of 285 in S/N ratio would be needed to include the three types of ocean water and a factor of 780 to include the first coastal type.

The minimum necessary S/N ratio for positive operation is shown separated into the safety factor and trigger bias. Other classes of communication systems not requiring a trigger bias or biased to a lesser degree have up to a factor of 6.8 available for use.

In daytime the background radiance can vary widely both as to spectral content and range of values. It changes, for example, with the sun's altitude, sea state, sky cover, and sea water type. For the present equipment, a study must be made of the behavior of the S/N ratios as a function of wavelength in order to determine the spectral regions of its optimum operation. The study was made of the most adverse case in order to determine the limit of system operation. Since spectral data on sea state effects are lacking, the attenuation of high seas, if any, cannot at present be included in this limit. Such a situation is found with the sun at its zenith on a clear day. Under these conditions, the sun will contribute over 80 percent of the irradiation (31) in the visible spectrum at the sea's surface. To determine the amount of radiation scattered upward, the quantity contributed by the sky will be neglected. In the erythema ultraviolet the sky may contribute as much as 50 percent of the total (32). The radiation contributed by each in the region between the visible and erythema ultraviolet is not known, but since only the ultraviolet region close to the visible is of interest, the amount due to the sky here will also be neglected.

Moon's data (33) was used to plot the spectral solar irradiance at sea level for one air mass and zenith sun (Fig. 24). For transponder-responder operation, it is seen that the amount of radiation scattered and reflected upward into the receiver is of importance.

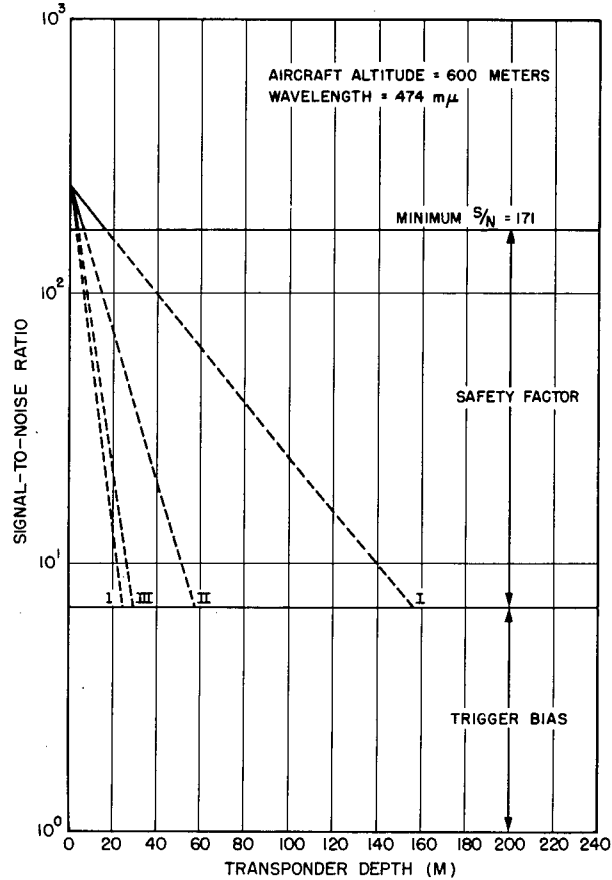


Fig. 23 - Daytime operation of present equipment acting as a transponder-responder section of an IFF system. A breakdown of the minimum S/N ratio required for positive operation is shown.

Spectral data on the radiation scattered upward are available only for Type I ocean water (4). From Fig. 25 it is seen that the backward scattering predominates in the blue-violet region and results in the blue color of the ocean waters. This backward scattering is fairly isotropic over a large solid angle. Consequently, the average value of the spectral radiant emittance (due to scattering) in the field or view of the receiver ought to be similar to the product of spectral values of Figs. 24 and 25. To this must be added the amount of sunlight and skylight specularly reflected toward the receiver. At zenith sun, roughly two percent of the incident sunlight radiation would be reflected vertically from a perfectly calm ocean at all wavelengths of interest. Of this, only that directly below the receiver would be reflected back to the receiver. Waves and turbulence will permit more of the sunlight in the field of view to be reflected into the receiver. Skylight, with its spectral content differing from sunlight and varying with zenith angle, will contribute reflected radiation from all parts of the field of view. The magnitude and spectral content of the combined radiation reflected toward the receiver are difficult to ascertain. The total is probably less than one percent of the incident radiation at any wavelength of interest here.

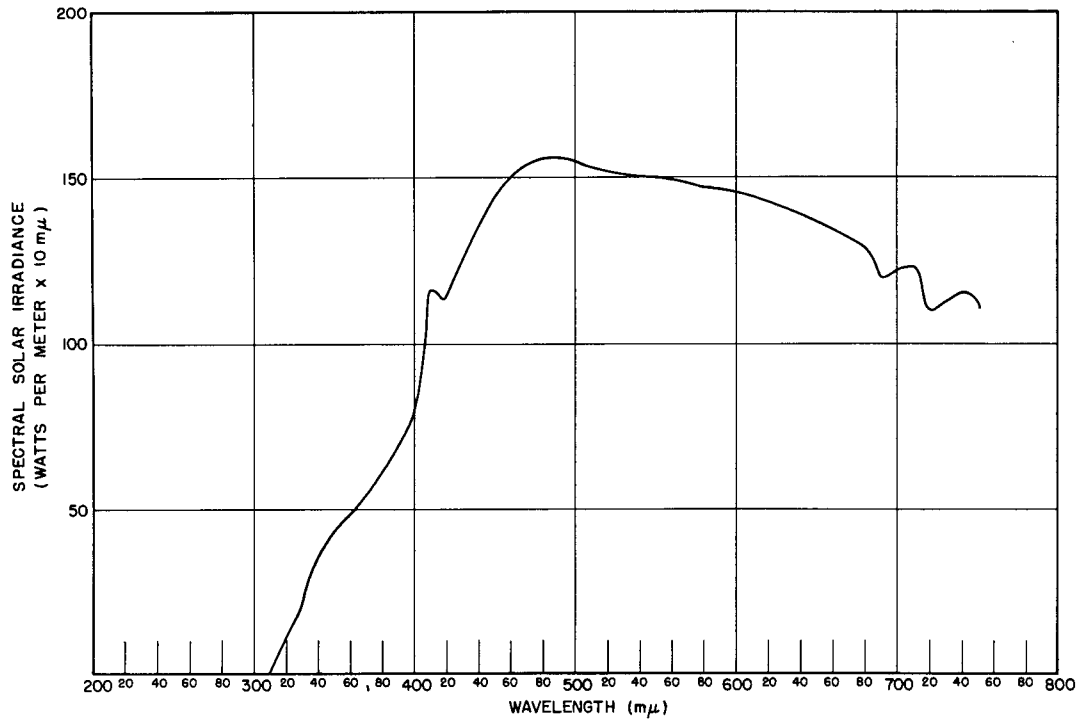


Fig. 24 - Spectral solar irradiance at sea level for one air mass and zenith sun

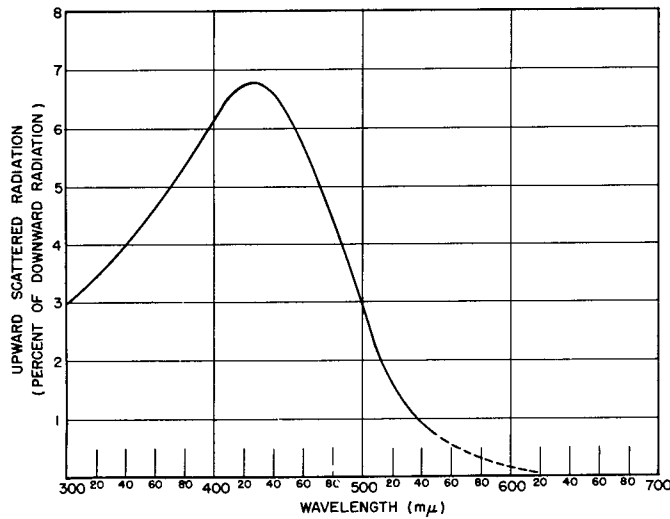


Fig. 25 - Upward scattered radiation for Type I ocean water--after Jerlov (Ref. 4). An extrapolation, indicated by the dashed curve, has been made at the longer wavelengths.

This is borne out somewhat by the work of Cox and Munk (18). Using red (Wratten A-25) filters in their aerial photography together with their theoretical considerations, they determined that roughly 50 percent of the background radiation (other than glitter) in the red region is due to scattered light, and the remainder comes from reflected skylight.

Daytime S/N ratios, which will be calculated without regard to the contribution from the reflected radiation, are expected to be approximately correct over the major portion of the given spectral region. For those regions where the amount of scattered radiation is small it must be realized that the calculated values of S/N ratios are too high.

All the parameter values used for this determination are those employed in the experimental equipment with the exception of the interference filter. The form of the filter used for these calculations (Fig. 26) approximates a shape that can be obtained commercially for any spectral region in which it is here used. Signal magnitudes are calculated for Type I ocean water with the transponder depth of 50 meters and an aircraft altitude of 600 meters. The integrals were evaluated at every $10\text{-m}\mu$ interval by using $5\text{-m}\mu$ bandwidths. In the noise calculation, the anode direct current was found from Eq. (18) with Moon's sunlight and Jerlov's scattering data both of which were used for obtaining the average spectral radiant emittance $W(\lambda)$ in the field of view.

The resulting S/N ratios (Fig. 27) are much too low for a workable system. The point of interest is their variation with wavelength. A maximum takes place at 440 millimicrons near the point where the greatest flashtube spectral intensity occurs, but otherwise there

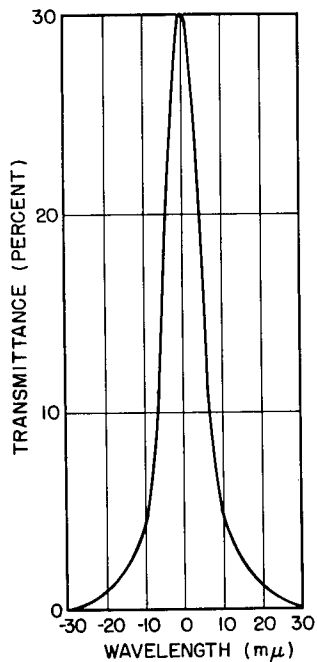


Fig. 26 - Transmittance of the standard interference filter used in the calculations

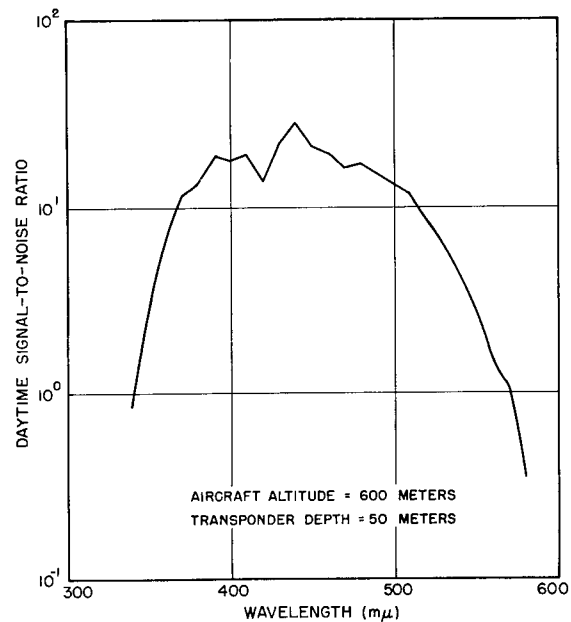


Fig. 27 - Variation of the daytime signal-to-noise ratios as a function of wavelength for Type I ocean water

is no significant difference in S/N ratios over a broad plateau extending from about 380 to 500 millimicrons.

Under similar circumstances, magnitudes of the S/N ratios are expected to be considerably lower for the other types of ocean water. Their distribution with wavelength will be changed not only by the difference in attenuation characteristics but by a shift of the scattered sunlight radiation. Knowledge of the latter effect for ocean waters other than Type I is not available in the literature. The optimum spectral region for operation in these other waters, however, should occur near the central region of the plateau of Fig. 27.

Some experimental evidence is available to confirm this statement. At a depth of 93.5 meters in Series 2 various interference filters were interchanged at the receiver. No signal was measurable at either 365 or 541 millimicrons. A comparison of S/N ratios at wavelengths where signals were obtained is as follows.

Wavelength (μ)	S/N
422	18
455	40
474	58

In the first two cases, the peak transmittance of the interference filters was almost a factor of two smaller than in the third. If the square root of this factor is applied to the third ratio, the S/N ratios can be obtained, in a rough manner, for comparison under identical parameters. The optimum region for daytime operation in Type II ocean water is then seen to fall near the center of the plateau.

Nighttime operation in the absence of moonlight characterizes the best conditions for IFF operation. In this case the current amplification (m) of the photomultiplier may be increased until the noise limit of the receiver is reached. When appropriate values of m and dark current \bar{I}_N have been substituted in, Eq. (5) should determine the noise limit for a particular tube. This manner of determining the noise has not been checked, but instead a method similar to the one used in daytime has been employed.

The daytime noise measurements were based on the number of spurious triggers occurring in a given time interval above a fixed trigger bias. Under these circumstances, the calculated and measured values of the rms noise in the anode circuit of the photomultiplier were in reasonable agreement for five microamperes.

If the dark current noise were pure Gaussian and if the noise triggered the oscilloscope at the same rate as in the daytime measurements, the rms values of the noise would be expected to agree in each case. This, however, has not been borne out. The measured rms value of the nighttime noise is a factor of six smaller than the daytime value, but the reason for this is not known. In both cases, oscilloscope displays of the noise show that although both are apparently random in nature the dark current noise contains some exceptionally high peaks. They are not peculiar to the particular tube used and are suggestive that the dark current noise is not purely Gaussian. The rms value, therefore, will not agree with the triggering rate. In the final analysis it is the triggering rate which forms the limit of the IFF system described here. For consistency, an "equivalent noise" is defined here for nighttime operation. Its value is taken as that of the calculated daytime

noise when the triggering rate of each is the same above a fixed bias. For the tube used throughout the experiments (m) was approximately 6000 when the equivalent daytime limit occurred.

The signal-to-noise ratios for operation in Types I and II ocean water are shown in Fig. 28. When the equivalent noise is used, the calculations are made in a manner similar to those used for daytime operations. The standard interference filter was used to eliminate the possibility of night sky light entering into the problem and to confine the region of operation, if this be needed for security reasons.

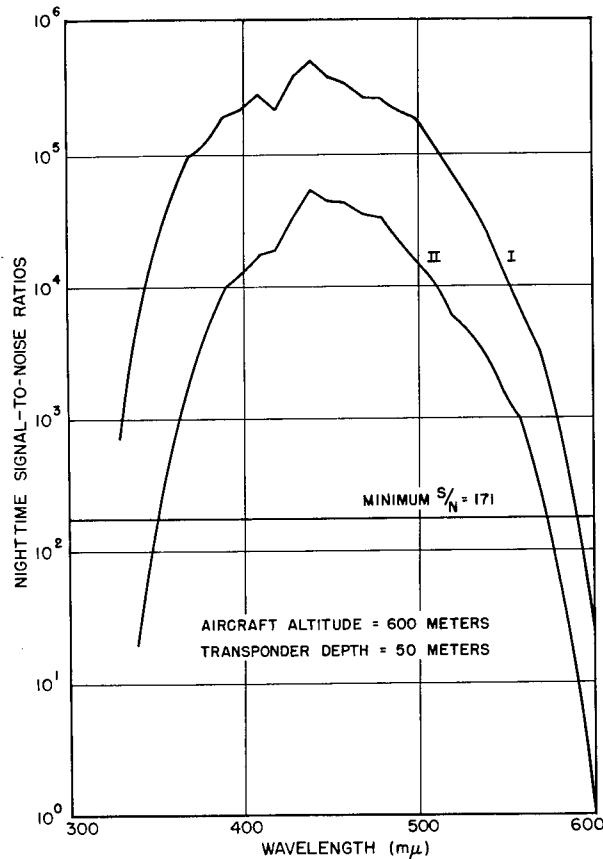


Fig. 28 - Variation of the nighttime signal-to-noise ratios as a function of wavelength for Types I and II ocean water

In the absence of moonlight, positive operation as an IFF system is possible over a large portion of the spectrum in both types of ocean water. Plateaus are not as broad as in daytime operation, but again the optimum region for operation occurs in the blue-violet portion of the spectrum.

If security dictates complete invisibility of the signals, operation must be restricted to the ultraviolet. Here the figure shows positive operation to be possible in both water types for the region between 350 and 400 mμ. Calculations have not been performed for

the third type of ocean water as yet, but since its attenuation is considerably more in the ultraviolet, the best region for positive operation in all three types when security is necessary would be as close to 400 $m\mu$ as possible. Even then added S/N ratios may be necessary to include the third type into a positive operating system and would certainly be needed to include the first coastal.

DISCUSSION

Under limited conditions, a nighttime IFF system is now believed to be feasible. For aircraft heights up to 600 meters and transponder depths down to 50 meters, either visible or invisible radiation may be used with success in the two types of clearest ocean water. Tentatively, the absence of moonlight is included as an additional restriction until measurements such as those of Stair and Johnston (34) can be applied to the problem. A rough calculation shows that an anode direct current due to a moonlit background would contribute significantly to the noise at a current amplification of 6000. The geographical regions of usefulness of the system are at present limited to tropical and subtropical ocean waters. The feasibility of the system in temperate and northern ocean waters remains to be studied. It is likely that positive nighttime operation in these waters could be achieved without much difficulty for either visible or invisible radiation.

Waters approaching the continents are classed by Clarke (16) as slope and coastal types. Little is known of the extent of their boundaries for most areas of the world. In his classification Clarke puts most of the waters off the northeastern United States as far out as 90 miles in a coastal class. A nighttime aircraft-submarine experiment in coastal waters and the slope waters that extend from the coastal type out to the Gulf Stream would serve a twofold purpose. First, it would establish the relationship between the classifications of Clarke and Jerlov and locate the boundaries of the different water types in the Northeast Atlantic. Second, it would be a direct check on the calculations made thus far.

The present equipment is incapable of positive operation as a daytime IFF system under any circumstances. Visual security is no problem in the daytime and consequently the optimum spectral region of performance may be used. To obtain positive operation in any of the three ocean water types, S/N ratios in the optimum region must be raised by a few hundred times. More is needed to include the other sea water types.

In attaining positive daylight operation, two somewhat different systems — one with a wide field of view and one with a narrow field — might well be investigated for military use. To cover large areas with fast low-flying aircraft, a wide field of view would be necessary. This system would be quite dependent on the zenith angle and would add an additional variable that should be studied quantitatively. If it were necessary to receive and transmit signals only in a small cone, a considerable increase in S/N ratios could be effected by the use of optics. Boettner and Barnett (35), using a 20-inch plastic Fresnel lens with a photocell receiver, increased signal gains as much as 350 times. Optical collectors as large as theirs may not be possible at the transponder, which must undergo considerable pressure, but some gain in this manner should be possible.

Whatever the optical system used there will still be a need for an additional S/N ratio, which must come from an increase in certain of the other parameters. It may also be possible to allow a larger anode direct current from the photomultiplier, thus realizing a small gain. Still, it is evident that a large portion of the necessary additional S/N ratio must come from an increase in signal intensity. Work on the problem of obtaining a higher flashtube peak output is being undertaken by the authors.

The findings of the present report apply equally as well to a communication system, the difference in the two being mainly one of repetitive rates. Only a minor gain in S/N ratio is realized by lowering the trigger bias. Faster flashing rates would also benefit the IFF system. The present rate is too slow to be of much use by aircraft and probably is suited only to the slow moving blimps. Obtaining higher peak intensities with faster flashing rates is therefore of prime importance in getting a positive operating system suitable for use under any circumstances.

ACKNOWLEDGMENTS

The authors are indebted to Dr. Donald M. Packer of the Optics Division for his assistance in obtaining the calibration of a 935 phototube, which was used in the determination of the flashtube spectral intensity distribution in absolute units.

* * *

REFERENCES

1. Plymale, W. S., Dawson, L. H., and Worsley, R. J., "Experiments on the Transmission of Ultraviolet Light in Chesapeake Bay Water," NRL Report 3774 (~~Secret~~), January 1951
2. Plymale, W. S., and Hansen, D. F., "Transmission of Ultraviolet Light Pulses in Sea Water," NRL Report 4021 (~~Secret~~), August 1952
3. Hulburt, E. O., "The Penetration of Ultraviolet Light into Pure Water and Sea Water," J. Opt. Soc. Amer., 17:15-22, 1928
4. Jerlov, N. G., Reports of the Swedish Deep-Sea Expedition 1947-1948, Vol. III, "Physics and Chemistry, Optical Studies of Ocean Waters," November 1951
5. Dawson, L. H., and Hulburt, E. O., "The Absorption of Ultraviolet and Visible Light by Water," J. Opt. Soc. Amer., 24:175-177, 1934
6. Tsukamoto, K., "Transparency of Seawater for Radiations in the Extreme Ultraviolet," Compt. Rend., 184:221-223, 1927
7. Saint-Guily, B., "Differences Des Coeff's D'Absorption de L'eau Pure et de L'eau de Mer, Prevues par la Theorie dans le Domain des Rayons X," Compt. Rend., 235: 893-894, 1952
8. Curcio, J. A., and Petty, C. C., "The Near Infrared Absorption Spectrum of Liquid Water," J. Opt. Soc. Amer., 41:302-304, 1951
9. Dorsey, N. E., "Properties of Ordinary Water Substance in all its Phases: Water-Vapor, Water, and all the Ices," New York: Reinhold, 1940. This book contains an extensive bibliography
10. Saxton, J. A., and Lane, J. A., "Electrical Properties of Sea Water," Wireless Engineer, 29:269-275, 1952
11. Rauen, T. J., "Underwater Radio," Report of NRL Progress (Quarterly ~~Secret~~ Supplement), 11-12, October 1953
12. Jerlov (Johnson), N. G., and Kullenberg, B., "On Radiant Energy Measurements in the Sea," Svenska Hydrograf-Biol Komm Skrifter 3:e ser hydrografi, Bd 1, H. 1, 1946
13. Kalle, K., "Zum Probleme der Meereswasserfarbe," Ann. d. Hydr. u. mar. Meteor. 66. H. 1, 1938
14. Poole, H. H., and Atkins, W. R. G., "The Penetration into the Sea of Light," Proc. Roy. Soc. (London), 123:151, 1937
15. Utterback, C. L., "Spectral Bands of Submarine Solar Radiation in the North Pacific," Conseil Perm. Int. p. l'Explor. de la Mer, Rapp.-Verb., v. CI, 2., 1936

16. Clarke, G. L., "Variation in the Transparency of Three Areas of the Atlantic Throughout the Year," *Ecology*, 20:520, 1939
17. Duntley, S. Q., "The Visibility of Submerged Objects," M.I.T. Visibility Lab., August 31, 1952
18. Cox, C., and Munk, W., "The Measurement of the Roughness of the Sea Surface from Photographs of the Sun's Glitter," *Scripps Inst Oceanog Reference* 52-61, AF Technical Report No. 2, Contract AF19 (122)-413, November 1952
19. Wright, W. D., "Photometry and the Eye," p. 118, London:Hatton Press Ltd., 1949
20. Stuart, L. E., "Identification, Friend or Foe Radars Sixth Sense," *Tele-Tech*, 6:60-67, January 1947
21. Hultgren, R. D., and Hallman, L. B., Jr., "The Theory and Application of the Radar Beacon," *Proc. I.R.E.*, 35:716-730, 1947
22. Rodda, S. C., "Photo-Electric Multipliers," London: MacDonal, 1953
23. Goldstein, E., "The Measurement of Fluctuating Radiation Components in the Sky and Atmosphere - Part 2 Final Results and their Application to Optical Communication," NRL Report 3710, July 1, 1950
24. Hynek, J. A., "Fluctuations of Starlight and Skylight," Ohio State University Research Foundation Project 480, Report No. 4, November 1952
25. Middleton, D., "Spurious Signals Caused by Noise in Triggered Circuits, *J. App. Phys.*, 19:817-830, September 1948
26. Dunkelman, L., "Horizontal Attenuation of Ultraviolet and Visible Light by the Lower Atmosphere," NRL Report 4031, September 1952
27. Huxford, W. S., and Olsen, H. N., "Electrical and Radiation Characteristics of Low Pressure Flash Discharges," Northwestern University, Dept. of Physics, Memorandum Report No. 29, September 1949
28. Oberg, E., and Jones, F. D., "Machinery's Handbook," p. 414, New York: Industrial Press, 1946
29. Goldman, S., "Frequency Analysis, Modulation and Noise," New York: McGraw-Hill, 1948
30. Huxford, W. S., et al., "Pulsed Infrared Systems," Northwestern University, Third Quarterly Progress Report (██████████), 1 February to 30 April 1953
31. Taylor, A. H., and Kerr, G. P., "The Distribution of Energy in the Visible Spectrum of Daylight," *J. Opt. Soc. Amer.*, 31:3-8, 1941
32. Luckiesch, M., Taylor, A. H., and Kerr, G. P., "A Four-Year Record of Ultraviolet Energy in Daylight," *J. of Franklin Inst.*, 228:425-431, 1939
33. Moon, P., "Proposed Standard Solar-Radiation Curves for Engineering Use," *J. of Franklin Inst.*, 230:583-617, 1940

34. Stair, R., and Johnston, R., "Ultraviolet Spectral Radiant Energy Reflected from the Moon," J. of Res. Nat. Bur. Stand., 51:81-84, 1953
35. Boettner, E. A., and Barnett, N. E., "Design and Construction of Fresnel Optics for Photoelectric Receivers," J. Opt. Soc. Amer., 41:849-857, 1951

* * *



DISTRIBUTION

CNO		
Attn: Op-374		1
Op-05W3		2
Op-316		3
Op-316C		4
Op-316D		5
Op-371C		6
Op-371M		7
Op-371U		8
Op-373		9
BuAer		
Attn: Code EL-46		10
Code EL-4323		11
ONR		
Attn: Code 466		12
Code 461		13
Dr. E. R. Piore, Code 102		14
BuShips		
Attn: Mr. C. S. Woodside		15
USNEL, Library		16 & 17
USNOTS		
Attn: Technical Library		18
USNUSL, Library		19
OCSigO		
Attn: Ch. Eng. & Tech. Div., SIGET		20
SCEL		
Attn: SCEL Liaison Office		21 - 23
ASTIA		
Attn: DSC-SD		24 - 28
Office of the Asst. Secretary of Defense (R&D)		
Attn: Technical Library Branch		29 & 30